World Scientific
www.worldscientific.com

JAPAN SOCIETY OF CIVIL ENGINEERS
COASTAL ENGINEERING COMMITTEE

Coastal Engineering Journal, Vol. 45, No. 4 (2003) 565–600
© World Scientific Publishing Company and Japan Society of Civil Engineers

RECENT DEVELOPMENTS IN THE GEOMORPHIC INVESTIGATION OF ENGINEERED TIDAL INLETS

DUNCAN M. FITZGERALD
Department of Earth Sciences, Boston University, 675 Commonwealth Avenue, Boston, MA 02215
dunc@bu.edu

GARY A. ZARILLO
Division of Marine and Environmental Systems, Florida Institute of Technology, Melbourne FL 32901
zarillo@fit.edu

SHELLEY JOHNSTON
Department of Earth Sciences, Boston University, Boston, MA 02215
shelleyj@bu.edu

Received 15 July 2003
Revised 27 October 2003

In recent years, numerous technological advances have made field studies and laboratory analyses of tidal inlets more time efficient while also substantially improved data quality. Mapping channel bathymetry was once a labor-intensive task that was accomplished by measuring water depths along a detailed network of channel profiles. Now aircraft-operated Light Detection and Ranging (LIDAR) can accurately map the bathymetry of most tidal inlets in a few hours' time. If greater detail of the channel bottom is required, then a multibeam acoustic system is utilized, although this technique is deployed from a boat and is less time efficient. The topographic version of LIDAR enables the construction of inlet shoreline maps and determination of volumes associated with shoreline gains and losses. In another advancement, side scan sonar mosaics now provide a picture of the bottom indicating different sediment types, bedrock outcrops, and bedform distributions. These surveys have also become essential for identifying scour holes next to rock jetties and assessing the susceptibility of these structures to collapse. The accretionary history and/or migrational trend of a tidal inlet can be determined from ground-penetrating radar transects on land and from shallow seismic surveys in water. These records provide a representation of the layers of sediment left behind as the inlet shifted positions. The hydraulic regime of a tidal inlet can be much more accurately determined using the Acoustic Doppler Current Profiler (ADCP). This instrument produces velocity profiles for an entire

inlet cross section and provides almost instantaneous discharges for small and moderately sized inlets. In a slightly different mode, ADCP technology has been used for directional wave measurements. Finally, significant upgrades in the manipulation of information, including Geographic Information System (GIS) and image analysis methods, have greatly facilitated the analyses and interpretation of the field data. These advancements have provided scientists with more effective means of gathering data, testing numerical models, and finding solutions to coastal engineering problems.

1. Introduction

Traditional geomorphic investigations of tidal inlets have attempted to produce conceptual models and predictive relationships that can be applied to inlets in similar physical settings. One successful approach in the investigation of tidal inlets has been through regression analysis of related morphologic and hydraulic characteristics. The most widely used of these relationships are Jarrett's (1976) refinement of LeConte's (1905) and O'Brien's (1931, 1969) correlation between tidal prism and inlet cross-sectional area, and Walton and Adam's (1976) correspondence between tidal prism and ebb-tidal delta volume. Since these early discoveries, several other useful predictions based on inlet tidal prism have been identified, including Shigemura's (1981) equilibrium throat width, Gibeaut and Davis's (1993) equilibrium ebb-tidal delta area, and Buonaiuto and Kraus's (2003) limiting depth over the ebb-tidal delta.

In addition to these quantitative relationships, numerous conceptual models have been presented that aid our understanding of tidal inlet processes. For example, net sediment transport through inlets has been inferred using a variety of data including migration and orientation of bedforms (Boothroyd and Hubbard, 1975; Hine, 1975; Zarillo, 1982; Zarillo, 1985; Sha, 1989; Fenster *et al.*, 1990; FitzGerald *et al.*, 2000, etc.), grain size distributions (Hubbard, 1975; Sha, 1990; Fenster and FitzGerald, 1996; FitzGerald *et al.*, 2002), velocity asymmetries (Dalrymple *et al.*, 1978; FitzGerald and Nummedal, 1983; Fry and Aubrey, 1990), and distortions of the tidal wave (Dronkers, 1964; Boon and Byrne, 1981; Speer and Aubrey, 1985). Models of barrier breaching and inlet formation have been proposed by Pierce (1967), FitzGerald and Pendleton (2002) and Kraus *et al.* (2003). Factors affecting channel geometry and rates of tidal inlet migration have been discussed by DeAlteris (1973), FitzGerald and FitzGerald (1977), and Kraus (1998). Processes governing shoreline recession and progradation have been identified at numerous inlets and are summarized in FitzGerald (1988, 1996). The pathways and processes of inlet sediment bypassing first recognized Bruun and Gerritsen (1959) have been further defined by FitzGerald (1988), Kraus (2000), and FitzGerald *et al.* (2001). These subsequent studies have also increased our knowledge of the cyclical pattern of channel switching and bar development at tidal inlets.

Despite the advancements in our understanding of tidal inlets, there are still difficulties in using traditional numerical and conceptual models because they are usually based on large populations and their predictive relationships do not provide for tidal

inlets that undergo cyclic changes. Conversely, some models have been established using very limit data sets and thus are too narrow in scope or insufficiently accurate to supply the quantitative information needed to solve problems for individual inlets. However, in recent years new technology has furnished the means to gather highly detailed and accurate topographic, bathymetric, hydraulic, and geophysical data during short time frames and over large geographical areas. These new instruments and means of compilation and analysis are producing far greater temporal and spatial predictability than has previously been possible. Armed with this new technology, scientists are poised to address long-standing coastal engineering problems, such as rates of bedload transport in tidal channels, modes of inlet sediment bypassing, processes of channel shoaling and migration, among many others. It is the purpose of this paper to describe how recent technology is advancing our knowledge of tidal inlet systems, including Ground-Penetrating Radar (GPR), bathymetric LIDAR, topographic LIDAR, shallow seismic surveys, multibeam bathymetric surveys, side-scan surveys, ADCP, and GIS manipulations.

2. Technological Advances

2.1. *Ground penetrating radar*

Ground-Penetrating Radar is a high-resolution geophysical technique, which is being successfully used in stratigraphic research of sedimentary environments including those associated with barrier island and tidal inlet settings boundaries (FitzGerald *et al.*, 1994; Jol *et al.*, 1996; van Heteren *et al.*, 1998). The instrument produces an "x-ray" view of the subsurface and provides a means of identifying and delineating sedimentary layers, bedrock horizons, the groundwater table, and buried structures. The system transmits electromagnetic (EM) waves into the ground having a frequency range of 10 MHz to 2000 MHz. The behavior of the EM waves and their depth of penetration are controlled by the electric conductivity, magnetic permeability, and dielectric permittivity of the sediments, which in turn is a function of moisture content, mineralogy, particle size, and salt water. As the instrument is dragged along the ground, EM waves penetrate the ground and energy is reflected back to the transreceiver differentially due to changes in the conductivity of the sediment. Sedimentary layers and other features in the subsurface are represented in the GPR records by reflectors that are interpreted based on their intensity, configuration, frequency, and continuity.

Ground-Penetrating Radar has been used to locate former tidal inlets as well as analyze the migrational patterns of existing inlets (FitzGerald *et al.*, 2001; FitzGerald *et al.*, 2002; Buynevich *et al.* 2003). Along the New England barrier coast the identification of paleo-tidal inlets has helped to assess the susceptibility of barrier systems to future breaching. For example, GPR profiles taken along the 8-km long Duxbury barrier on the Massachusetts south shore revealed the position of 18 former tidal inlets. The existence of these inlets not only demonstrates the vulnerability of

this barrier to future storms but the distribution of the inlet fill sequences aided in the delineation of hazard zones (Fig. 1; FitzGerald *et al.*, 2001). The migrational patterns and infilling characateristics of the paleo-inlets as imaged in the GPR records also helped to determine historical patterns of longshore sediment transport along Duxbury Beach. At Wells Inlet on the southern Maine coast, GPR data corroborated paleo-inlet shoreline positions. Additionally, the fillets on both sides of jettied entrance were shown to have formed from beach progradation due to the sequestration of sand from the littoral transport system (Montello, 1992). At another site on the central Maine coast accretionary patterns observed in GPR profiles at the mouth of Kennebec River document that the inlet had narrowed and deepened as the channel cross section reached a state of dynamic equilibrium (Fig. 2; FitzGerald *et al.*, 2002). These examples illustrate that GPR is a valuable tool for deciphering inlet shoreline histories. The portable nature and ability to collect data rapidly make GPR an ideal instrument in the field investigation of tidal inlets. One drawback in the use of GPR is that saltwater attenuates the EM signal and thus it cannot be utilzed near saltmarsh environments or close to the ocean or bay shorelines.

2.2. *Topographic lidar*

LIDAR surveys offer an efficient way to collect data with centimeter accuracy over large areas. Collected from an aircraft, laser pulses are transmitted and then the return signal is recorded. The time lapse between the transmitted and return signal is used to calculate the distance from the plane to the ground. The elevation can then be calculated because the plane's location is simultaneously recorded with a Kinematic differential Global Positioning System (GPS). From an altitude of 1,000 m, data can be collected at 2,000 to greater than 200,000 points per second (Brock and Sallenger, 2001). Typical accuracy is ±10–15 cm vertically and ±1 m horizontally (Brock and Sallenger, 2001). NASA's Airborne Topographic Mapper (ATM) collects elevation points every few meters that are ±14 cm (Sallenger *et al.*, 1999).

LIDAR data is extremely helpful when working on regional scale projects, such as barrier island and flood plane mapping, regional sediment management projects, and storm assessment, because the data are collected much more quickly than with conventional survey techniques (Brock and Sallenger, 2001). Assateague Island ($\sim$ 100 km) was mapped in approximately 3 hours (Krabill *et al.*, 2000). Another survey to assess storm damage after Hurricane Opal along the pan handle of Florida was completed in just over 2 hours. A conventional survey of the same area had previously taken 6 months to complete (Bolivar *et al.*, 1995). Vegetation structure can also be described by analyzing multiple return signals (Blair *et al.*, 1999). This example illustrates how effectively LIDAR can be used to map large shoreline segments and determine the impact of major storms.

LIDAR data collected from tidal flats in Humboldt Bay, Humboldt, CA were added to the circulation model for the Bay. The Bay is 70% tidal flats that are

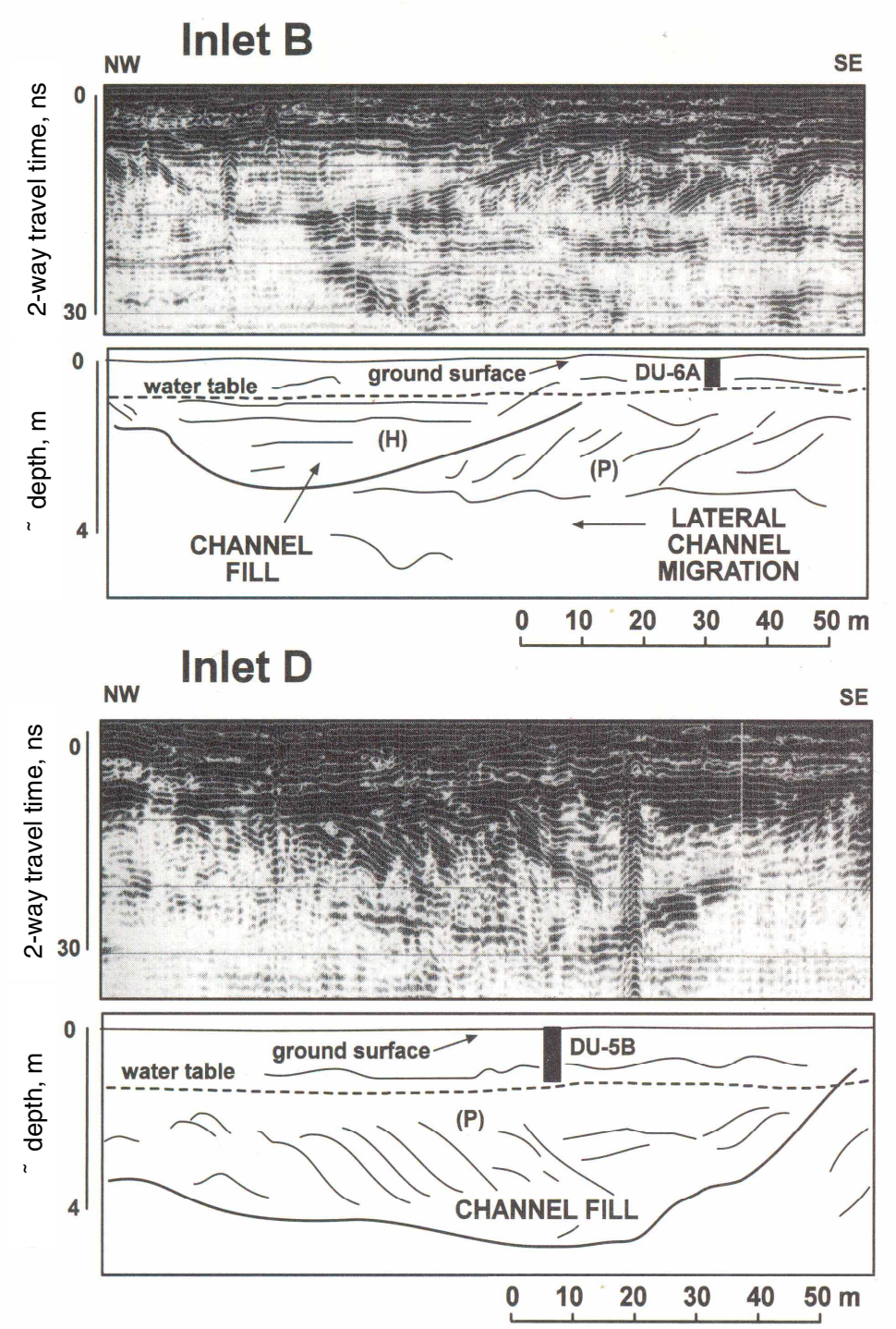

Fig. 1. GPR sections and interpretations of fomer tidal inlet sites along Duxbury Beach, Massachusetts. The reflectors provide a means of interpreting the processes of channel infilling and paleo-longshore transport directions (from FitzGerald *et al.*, 2002).

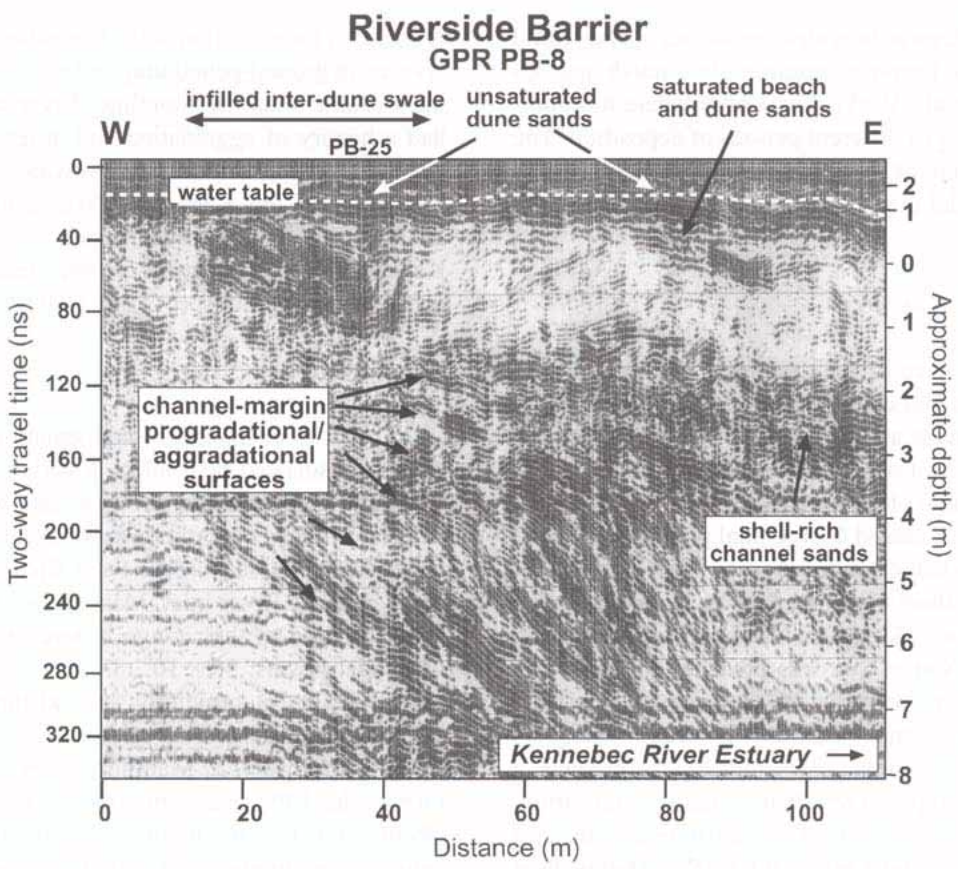

Fig. 2. GPR record of Riverside Beach, which forms the border to Kennebec River Inlet on the central Maine coast. The pattern of reflectors demonstrates that the channel has narrowed as the inlet has reached an equilibrium cross sectional area (from FitzGerald *et al.*, 2002).

exposed at low tide (Costa and Glatzel, 2002). These areas were inaccessable by boat for traditional boat surveys and were difficult to access by land. The LIDAR survey provided detailed elevation data and improved the results of the hydrodynamic circulation model (per. comm. Adele Militello).

In the fall of 1995 and the spring of 1996, Assateague National Seashore was mapped with the ATM (Krabill *et al.*, 2000). The LIDAR surveys were compared to conventional ground surveys in order to estimate the accuracy of the LIDAR survey. The error was estimated as the difference between the elevation of the ground survey and any LIDAR point falling within one meter of the ground survey transect. The LIDAR survey was collected in November 1995 and the ground survey was collected that September. The mean error ranged from 0.01 to 0.15 metres. The average error for all 10 transects was 0.06 metres.

LIDAR surveys have also been used on the West Coast to document a range of geomorphic responses to the 1997–1998 El Niño. Locally, some cliff locations

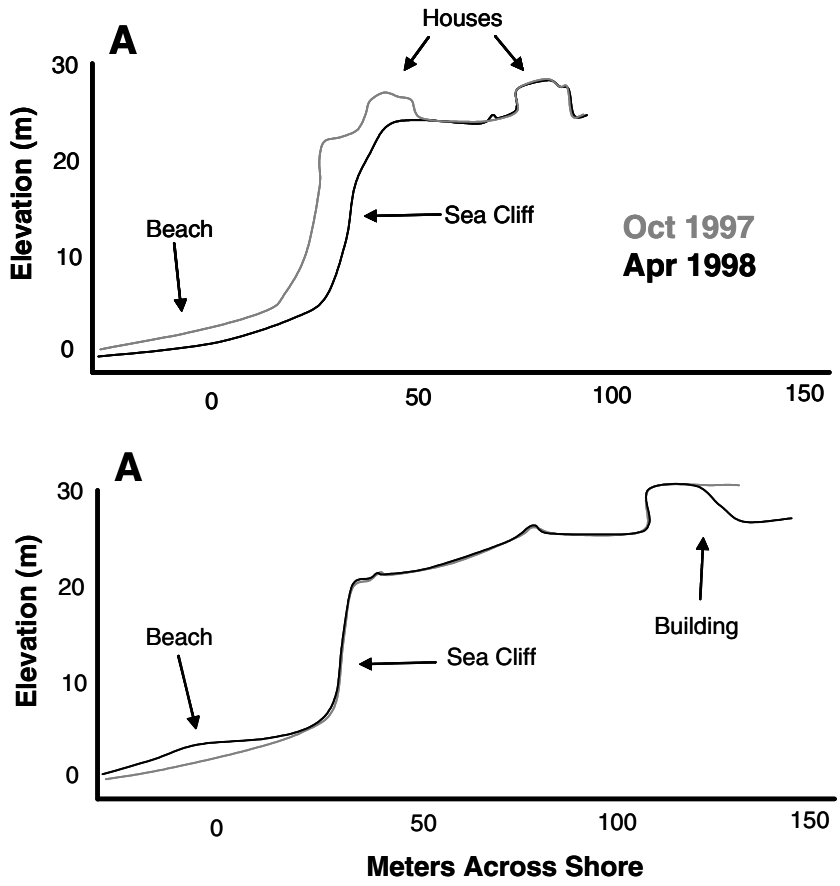

Fig. 3. Cliff erosion documented by LIDAR surveys (after Sallenger *et al.*, 1999).

remained stable while other areas eroded between 10–13 m (Fig. 3) (Sallenger *et al.*, 1999). Spatial variability in cliff response maybe related to the changes in the beach at the base of the cliff (Sallenger *et al.*, 1999). For example, areas experiencing cliff erosion are also expected to be experiencing beach erosion. Removal of beach material will make the cliff vulnerable to toe erosion, mass slumping, and subsequent cliff retreat. This type of study illustrates the potential for correlating cliff erosion to adjactne beach processes though LIDAR mapping.

2.3. *Bathymetric lidar*

LIDAR survey techniques have been expanded to facilitate the collection of bathymetric data. Bathymetric LIDAR surveys provide a means of collecting regional scale bathymetric data in order to manage coastal projects from a regional perspective. This regional approach was taken in the northern Gulf of Mexico where 265 km of shoreline were surveyed in Florida and Alabama in order to evaluate the benefits of regional sediment management (Parson, Lillycrop, and McClung, 1999).

One bathymetric LIDAR survey system, the SHOALS (Scanning Hydrographic Operational Airborne LIDAR Survey) system, was developed by the United States Army Corps of Engineers (USACE) and has been operational since 1994 (Irish and Lillycrop, 1999). The SHOALS system works by transmitting a two simultaneous laser pulse from a plane, one infrared and one green. Two return signals are recorded — the first, the infrared signal from the water's surface and the second, the green from the seafloor (USACE 2001). Water depth is determined by the time lapse between the two signals. The operational depth of the SHOALS system is limited by water clarity and substrate type. Generally this is not more than 40–60 m or 2–3 times the Secchi depth (Irish and Lillycrop, 1999, Parson, Lillycrop, and McClung, 1999, USACE 2001). The SHOALS system also has the capability to map subaerial areas. The SHOALS system conforms to USACE Class 1 and International Hydrographic Organization Standards (Riley, 1995). The vertical accuracy of the SHOALS system is ±15 cm and the vertical accuracy is ±3 m with differential GPS and ±1 m with Kinematic GPS (Irish and Lillycrop, 1999, USACE 2001).

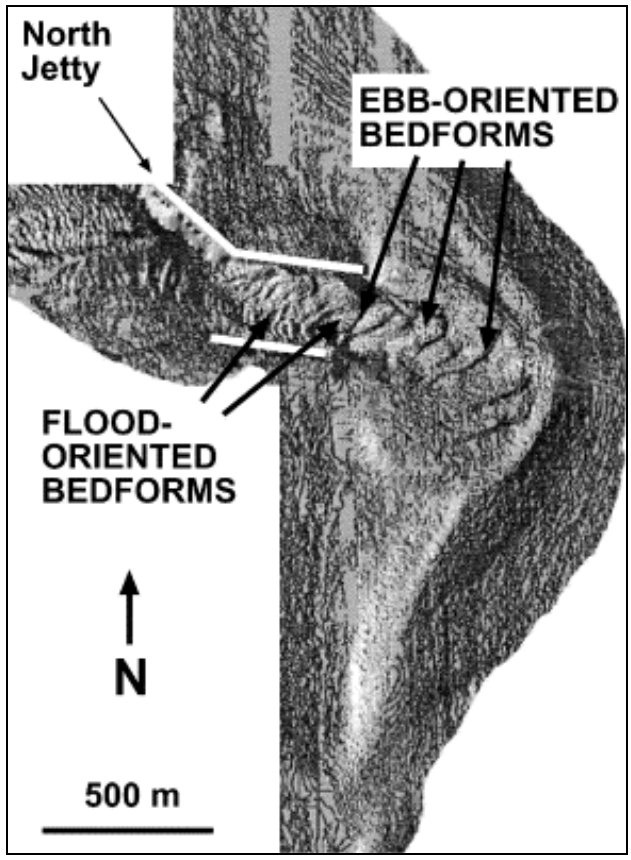

Fig. 4. LIDAR survey of Merrimack River Inlet ebb tidal delta. Note the large sandwaves that are migrating seaward in the main ebb channel (from FitzGerald *et al.*, 2002).

Merrimack River Inlet is a riverine-associated inlet (FitzGerald *et al.*, 2002). The sediment supply to this inlet is dominated by an influx of fluvial sediment during late winter and early spring freshets. Bathymetric LIDAR data collected by the USACE clearly displays ebb-orientated sandwaves and flood-oriented megaripples (Fig. 4; FitzGerald *et al.*, 2002). Based on the LIDAR information gathered in this study, sediment transport is determined to be seaward.

SHOALS surveys were collected three times during 1994 at New Pass, Florida in March, September, and December (Irish and Lillycrop, 1997). The spatial extent of these surveys varied but in total the channel, ebb delta, and adjacent nearshore areas were covered. Expansion of the survey area from the navigation channel to the surrounding areas provided a more complete explanation of the morphological changes. Not only could the erosion and shoaling within the navigation channel be explained by the sequential surveys but sand sources and sinks could also be identified. The SHOALS surveys demonstrate that the cause of shoaling along the north side of the ebb tidal delta was due primarily to sand influx from longshore sediment (Fig. 5; Irish and Lillycrop, 1997).

Bathymetric LIDAR surveys have also been applied to the study of the effects of coastal structures. Preaque Isle in Lake Erie is a 10-km long recurved sand spit (Mohr, Pope, and McClung, 1999). It has 55 segmented breakwaters to protect it from erosion (Mohr, Pope, and McClung, 1999). In 1995, a SHOALS survey was added to the monitoring strategy and extend from the subaerial beach to a depth of about 7 m (Mohr, Pope, and McClung, 1999). Volume analysis of the SHOALS surveys showed an accretionary trend between the breakwaters and the shoreline while there was erosion seaward of the breakwaters. Seaward of the breakwaters resulted in the seafloor being lowered an average of 0.2 to 0.4 m over the four year monitoring period (Mohr, Pope, and McClung, 1999).

2.4. *High resolution shallow marine seismic surveys*

Seismic reflection profiles provide an image of the subsurface and are particularly useful for delineating sedimentary layers, bedrock outcrops, depth to the acoustic basement, and other geological features beneath the sediment-water interface. Traditionally, seismic surveys have been employed to help determine the stratigraphy and evolution of various depositional sequences on the continental shelf and in nearshore settings such as estuaries, lagoons, and major river channels. In recent years seismic surveys have been utilized at tidal inlets to decipher channel migrational trends and overall depositional history of the inlet (Buynevich *et al.* 2001), dredging requirements (FitzGerald and Montello, 1990), and thickness of ebb-tidal deltas (FitzGerald and Nummedal, 1977). High resolution seismic equipment produces acoustic waves using a variety of sources including boomer systems, sparker arrays, or air gun. Depending upon the desired imaging, particular energy outputs and filtering schemes are used; lower frequencies noise produces greater penetration,

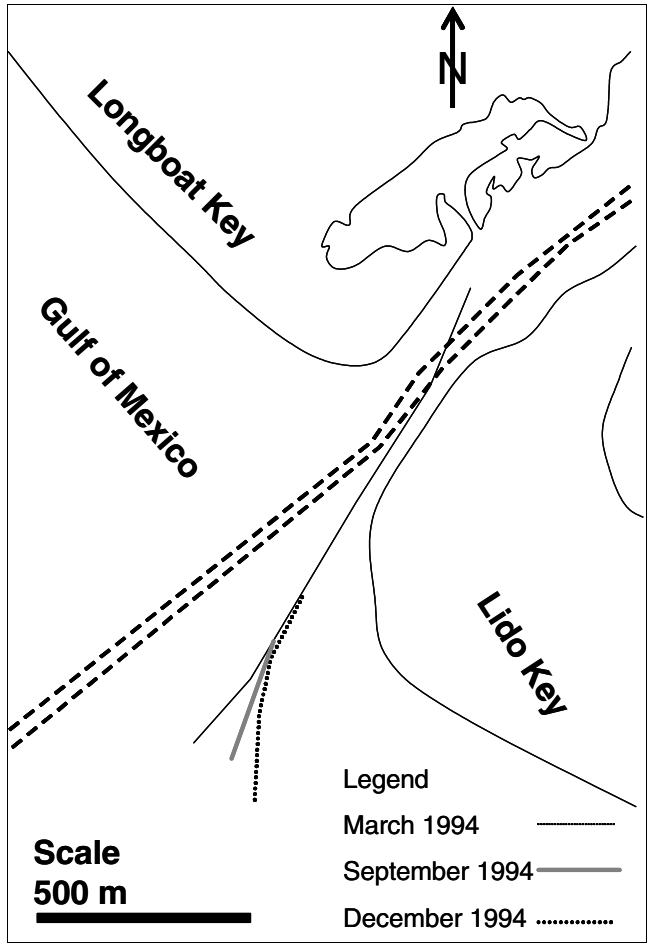

Fig. 5. Migration of inlet thalwag at New Pass, Florida (from Irish and Lillycrop, 1997).

whereas higher frequencies yield better resolution. A recent advance in sub-bottom seismic technology is the frequency swept or Chip system. Chirp technology reduces the trade-off between signal range and image resolution. The Chirp system's bandwidth, as well as frequency determines the spatial resolution. The Chirp swept frequency sonar system emits a broadband FM source pulse having low frequencies for depth penetration into the sub-bottom and higher frequencies for high vertical resolution. The typical Chip data acquisition unit controls all data transmission, recording and signal processing including analogue to digital conversion, compression of the FM pulse and spherical divergence correction. The recorded signal is the output of the correlation filter used for pulse compression and is usually stored in industry standard SEG-Y format.

A series of hydrophones trailed behind the boat receives the return signal. Similar to GPR, energy that penetrates the sediment is reflected off changes in lithology

producing an image of the subsurface sediment layer, bedrock surface, or other feature. Interpretation of the seismic records relies not only on a knowledge of the velocity of (acoustic) waves in common earth materials, but also on a well-defined set of reflection patterns (Mitchum *et al.*, 1977). Like GPR records, most seismic reflection patterns are not uniquely tied to a single sedimentary environment, creating the need for comprehensive sets of seismic facies and interpretations for each depositional setting.

Along France's Atlantic coast, Bertin *et al.* (in revision) used a detailed network of shallow seismic profiles to determine the depositional history of Maumusson Inlet. They showed that a recent increase in sedimentation in the backbarrier led to a smaller bay tidal prism. The inlet channel responded to the reduced tidal prism by shoaling and shifting southward. The seismic records not only established the pattern of channel infilling, but also demonstrated how the shoaling of the channel facilitated migration of the thalweg out of its bedrock-cut valley. Similar geophysical work by Buynevich *et al* (1999) along the coast of Maine traced the evolution of Kennebec River inlet using high resolution seismic profiles. These investigators speculated that a slowing of sea-level rise and a stabilization of the inlet tidal prism resulted in closure and significant shoaling of secondary entrance channels. Seismic data documented that two of the former estuarine channels were more than 50 meters deep (Fig. 6; Buynevich *et al.*, 1999).

Shallow seismic surveys provide a means of studying the development of tidal inlets prior to historical documentation. The pattern of subsurface reflectors observed at tidal inlets can be related to channel cut and fill, inlet migration, erosional and depositional trends, bedrock controls, and other inlet and geological processes. At most tidal inlets surveys can be completed in a day or two and sophisticated post-processing programs greatly facilitate data analysis and interpretations.

2.5. *Multibeam*

Multibeam technology was originally developed in the 1960s by the US Navy for deep water bathymetric mapping (USACE 2001). This technology was extended and has been available for use in shallow water environments since the early 1990s (USACE 2001). Detailed coverage is helpful for ensuring navigation safety, morphologic analysis, and evaluation of underwater structures (USACE 2001, Prickett 1996). Multibeam surveying is based on the return time of many acoustic signals transmitted simultaneously. The timing, phase, and amplitude of the return signal will depend on the depth of the seafloor, bottom reflectivity, and slope angle of the incident beam (USACE 2001). Surveys collected by a multibeam system provide essentially continuous coverage of the seafloor, although the exact coverage will depend on the configuration of the system and water depth. Spacing of individual beams in the transducer head range from 0.5 degrees to 3.0 degrees (USACE 2001). Potential errors, such as vessel roll, pitch, and yaw, and time lag between the positioning

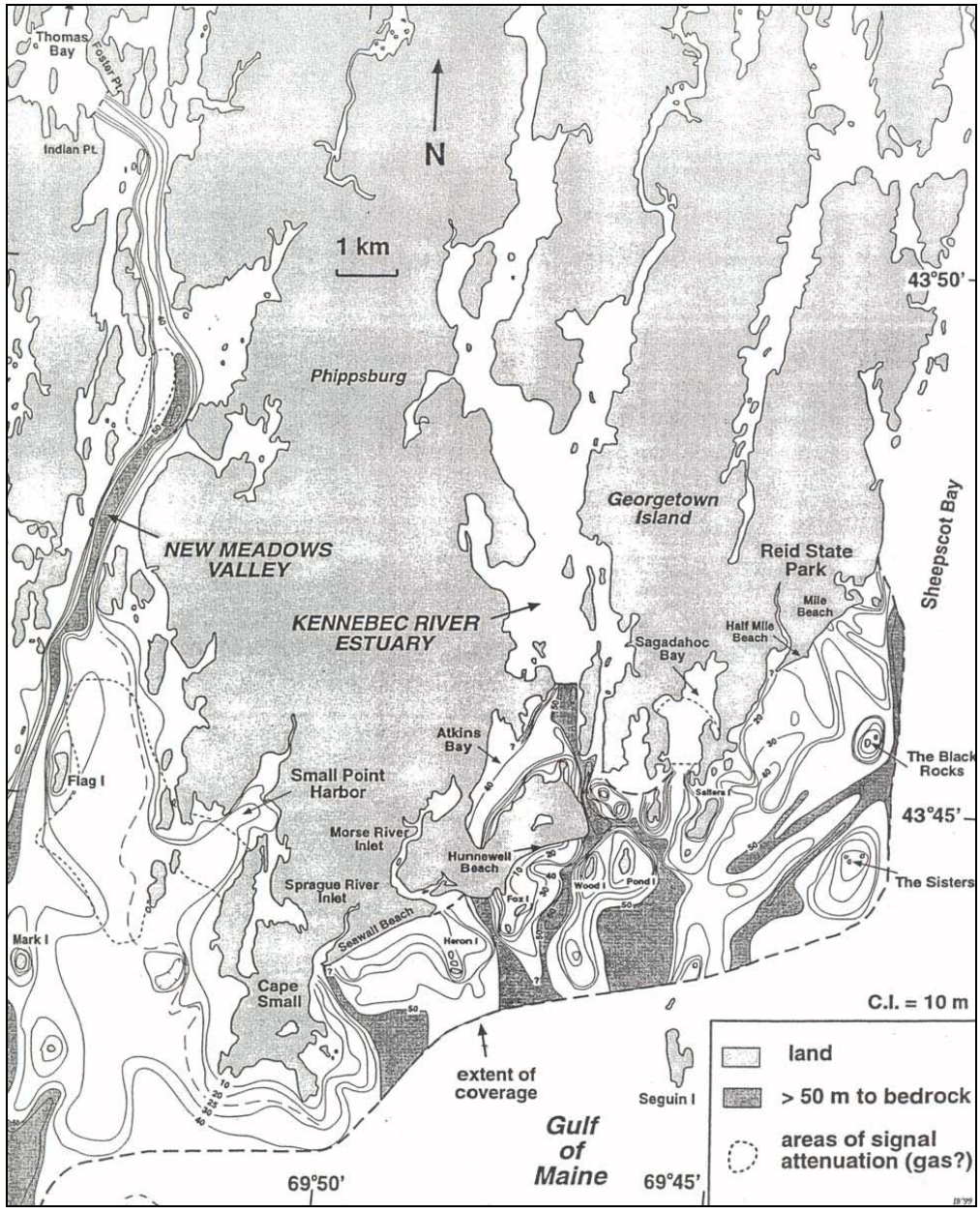

Fig. 6. Structure contour map of the depth to acoustic basement (in meters) that was produced from a detailed shallow seismic survey of the area. The map identifes former entrance channels occupied by the paleo-Kennebec River, Maine (from Buynevich *et al.*, 1999).

sensor (GPS) and the sonar measurement, are recorded with on board instrumentation and incorporated into the post-processing procedure (USACE 2001). Care must be taken to prevent/minimize other errors such as inaccurate alignment of sensors, transducer draft depth, and sound velocity measurements (USACE 2001).

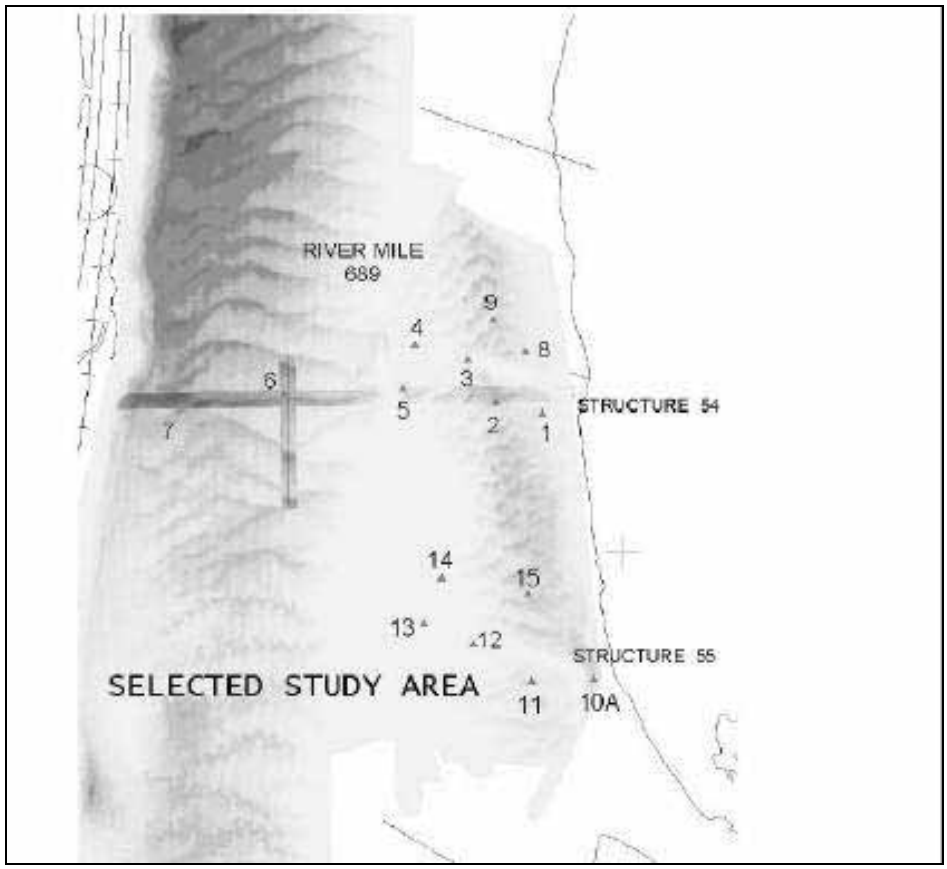

Fig. 7. Multibeam survey form the Mississippi River. Scale was not in oridinal publication (from Abraham and Pratt, 2002).

Multibeam surveys have been used on the upper Mississippi River to evaluate the performance of navigation structures (Fig. 7). These surveys were also used to estimate the bedload transport in the river using the Integrated Surface Difference Over Time (ISDOT) technique (Abraham and Pratt, 2002). With this technique the bedload transport is calculated from the change in the elevation of the river bottom measured from sequential multibeam survey covering the same spatial extent. For this calculation, three surveys were collected. The surveys have time laps of 2.3 and then 4.8 hours. The bedload estimate for this area was 0.0041 kg/sec/m (Abraham and Pratt, 2002).

Morphologic analysis of Egmont Channel in Tampa, Florida, used multibeam data collected in 1999 and 2001 (Narr *et al.*, 2003). These surveys identified large subaqueous dunes in the north and west with medium sized dunes superimposed on top of the larger ones (Fig. 8; Narr *et al.*, 2003). The large dunes migrated 13 m to the west northwest (Narr *et al.*, 2003). In the deepest part of the channel were smaller sandwaves.

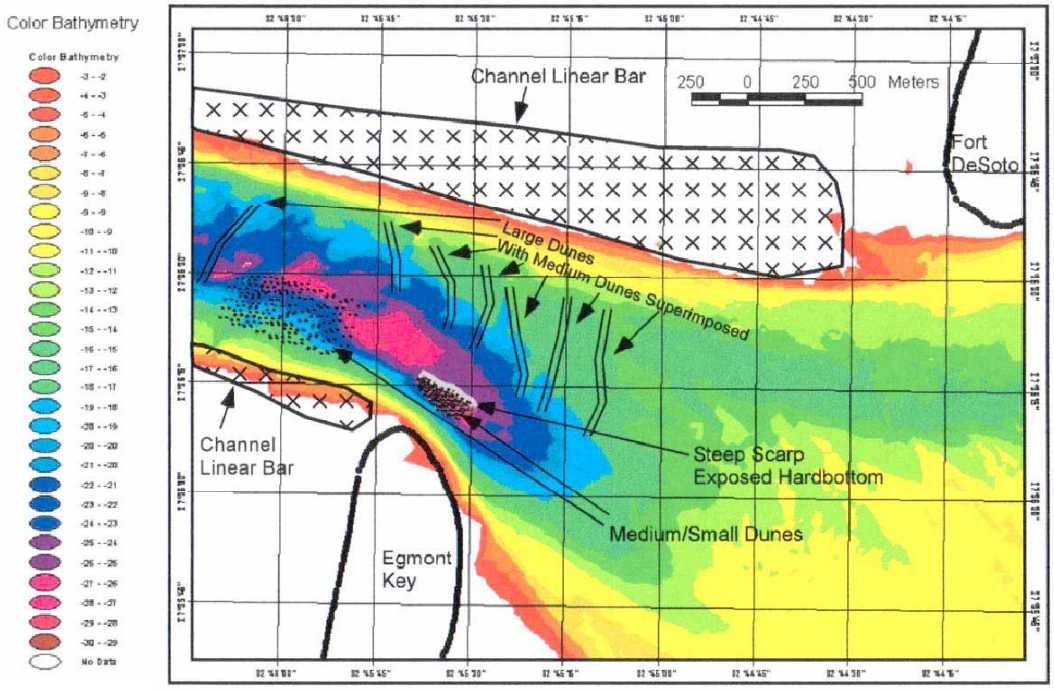

Fig. 8. Egmont Deep, Tampa, Florida (from Narr *et al.*, 2003).

2.6. *Side scan sonar*

Side scan sonar is a method of imaging the ocean floor whereby a "picture" of the bottom is obtained on both the port and starboard sides of the ship's track (Fig. 9). The technique is similar to radar, but uses sound echoes instead of electromagnetic pulses. A towfish transmits narrow beams of acoustic energy (sound) at a wide angle across the sea floor. High frequencies, such as 500 kHz to 1 MHz, give excellent resolution but the acoustic energy travels a short distance. Lower frequencies such as 50 kHz or 100 kHz provide lower resolution but the travel distance is greater. The acoustic energy is reflected off objects on the bottom and back to the towfish. The intensity or strength of the returning acoustic signal is controlled primarily by the slope of the seafloor as well as by its composition. A stronger return is received if the seafloor slopes toward the instrument or if the seafloor is made of bare rock. The strength of the return is much lower if the seafloor consists of mud or sand. Hard objects reflect more energy causing a dark signal on the image and soft objects reflect less energy producing lighter signals. The absence of reflected energy, such as the shadow behind an object, shows up as a white area on a sonar image.

At tidal inlets side scan surveys are employed to map the consistency of the channel bottom and identify bedrock outcrops. The maps are usually ground-truthed using grab samples and vibracores. Bedrock and gravel bottoms produce sharp

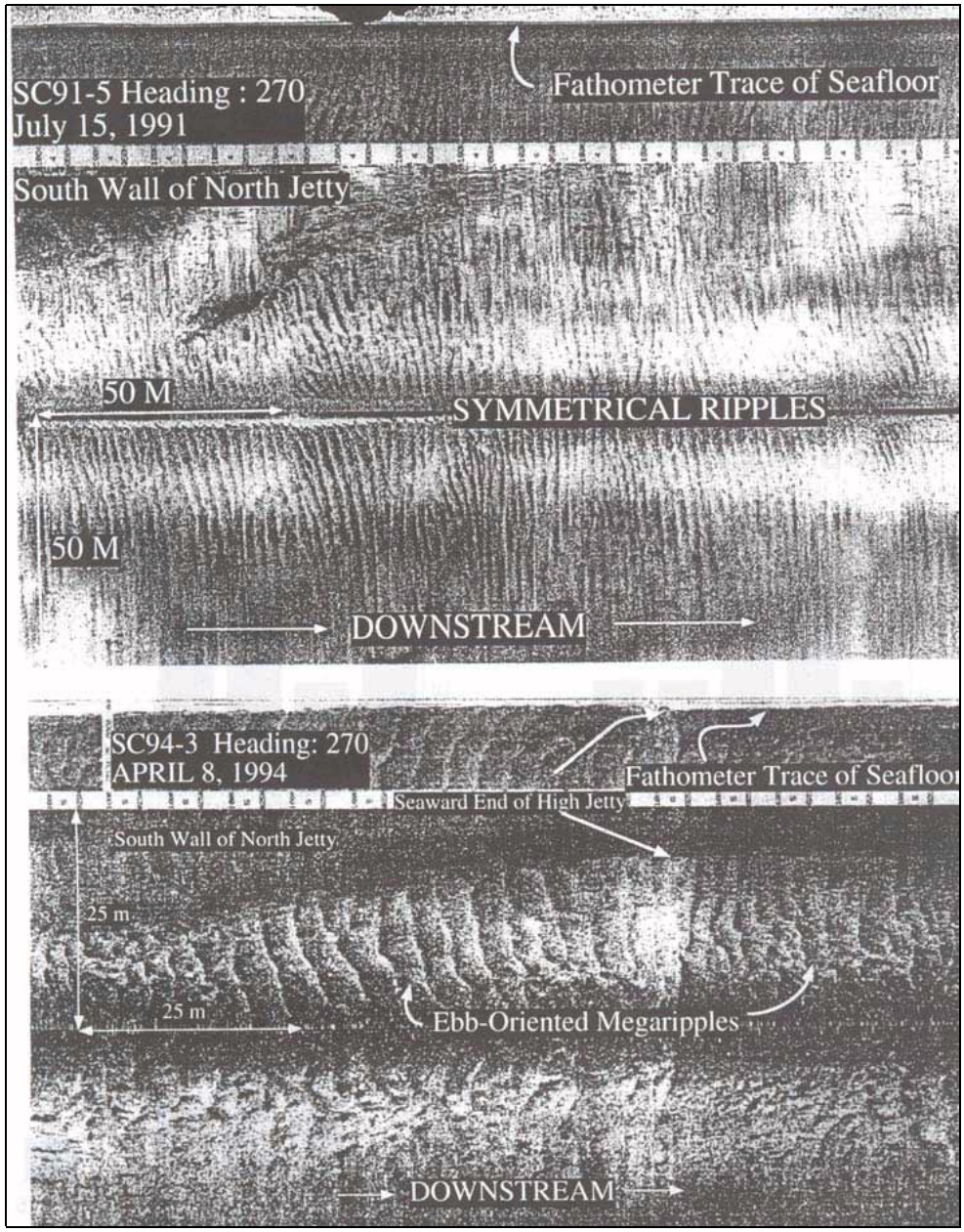

Fig. 9. Side Scan survey record of the jettied entrance of Saco River Inlet. The top survey was taken during average tidal conditions whereas the bottom record (same channel region) was taken during high freshwater discharge conditions. Correspondingly, the bedforms changes from symmetrical ripples to ebb-oriented megaripples (from Kelley *et al.*, 1995).

images, whereas sand yields weaker images and mud even weaker images. Side scan surveys are also performed adjacent to coastal structures such as rock jetties to determine areas of possible undermining and assess their vulnerability to collapse. These maps provide a clear picture of scour holes and can even image individual boulders dismantled from the structure. These surveys are most beneficial when done in conjunction with multibeam surveys.

One of the clearest means of identifying pathways of sediment movement through inlets and determining net bedload sediment transport directions in tidal inlet channels is by monitoring large bedforms and mapping their orientation. Side scan sonar mosaics can provide a detailed bedform map of the channel bottom and can be used as a first order assessment of sand transport calculations based on hydraulic data. An indication of.the usefulness of side scan technology is shown at the jettied entrance of Saco River Inlet (Fig. 9). The two images in Fig. 9 were taken in the same area of the channel and demonstrate how the channel bottom responds to changing flow conditions. Similar maps have been used at other inlet to monitor the migration of large sandwaves into navigation channel (Fenster and FitzGerald, 1996).

2.7. *Acoustic doppler current profiler technology*

2.7.1. *General use*

The Acoustic Doppler Current Profiler sensors use the Doppler effect to measure current speed. In this case the Doppler shift is a change of frequency of a sound wave when reflected from an object moving with a relative speed to the sound source. ADCPs use the Doppler effect by transmitting sound at a fixed frequency and measuring the backscatter returned from small particles present in the water (small particles of sediment and organic matter). It is assumed that these particles move with the same horizontal velocity as the water. The modern acoustic Doppler current profilers are profiling current meters that can measure current speed and direction in several spatial bins though the water column or across a channel. Its predecessor was the Doppler speed log that measured the speed of ships through the water or over the sea bottom at shallow waters. A redesign of the speed log to measure more accurate velocity over a depth profile resulted in the first VM-ADCP in the 1970s. ADCP technology advanced in the 1980s with the development of different ADCP models (self-contained, vessel mounted, and direct reading). Doppler signal processing has evolved over the years. Relatively simple processing algorithms with phase locked loops have been used in speed logs.

In the first generation of ADCPs a narrow-bandwidth, single-pulse, autocorrelation method was used to extract velocity information. Broadband ADCP technology was developed in the early 1990s. Narrowband ADPCs measure frequency shifts of single sound pulses. Broadband ADCPs measure phase shift of multiple echoes over a broad range of frequencies. Each broadband sound pulse contains shorter coded pulses. The phase ambiguity is resolved by autocorrelation methods.

Broadband Doppler phase processing is equivalent mathematically to the Doppler shift of frequency. Broadband ADCP technology has proven to be an accurate method that enables ADCPs to take advantage of the full signal bandwidth available for measuring velocity. The result of a 100 times increase in acoustic frequency bandwidth is velocity measurements with 10 times better accuracy than with narrowband ADCP. The accuracy of the current velocity measurements is typically a few centimeters/second.

Figure 10 schematically shows the configuration of a bottom mounted ADCP with respect to the water column. Current information is obtained in depth cells that are regularly spread in a grid covering the volume that is measured with the

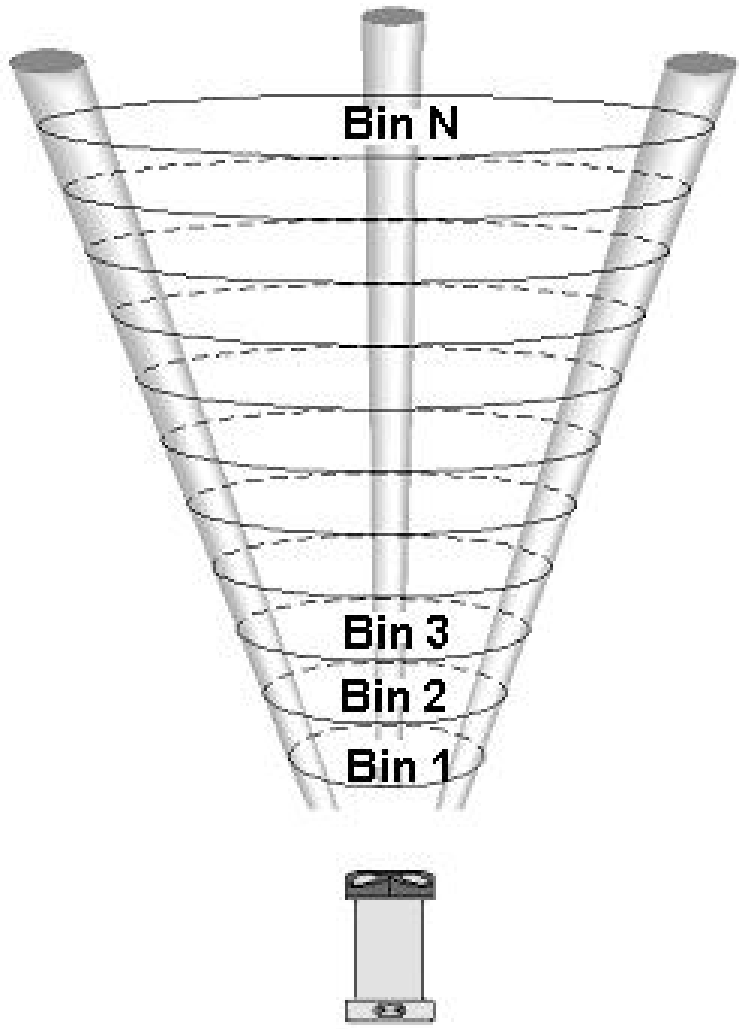

Fig. 10. Schematic view of bottom mounted ADCP configuration used to measure current velocity in a series of vertical bins through the water column.

Table 1. Operation range of commercially available ADCP technology.

Frequency (kHz)	Bin Size (m)	Range (m)
1200	1	19
600	2	67
300	8	165

Table 2. Coastal, inshore and nearshore ADCP deployment configurations.

Water Depth	Moving Deployment	Fixed Deployment
Surface	Coastal vessel	Buoy — mooring (waves)
Mid-depth	Towfish	Horizontal mooring
Bottom	ROV/AUV	Bottom fram

ADCP. The ADCP gives the average velocity vector over each cell. A weight function is applied, so that the signal in the center of each cell has more weight. Data produced by a broadband ADCP includes current velocity in Earth coordinates, echo intensity (depends on sound absorption, beam spreading, transmitted power and scatters), correlation coefficient (depends on data quality), and percent good parameter (depends on correlation coefficient and vertical error velocity). The length and range of the pulses (pings) are limited by the operating frequency. The pulse length determines the minimum cell size. Table 1 lists the typical operating frequencies of commercially available ADCP units along with the minimum cell size and range associated with each frequency range. Single-ping random errors are relatively large. Therefore, time averaging is required for reliable measurements. Typically an averaging period lasts 1 minute or longer. During this period, ADCP data are logged along with navigation data. Conversion of ADCP measurements to absolute current velocities is typically performed afterwards with post-processing, but they can also be processed on-line.

2.7.2. *Shallow water current meters*

ADCP measurements have been extensively used to quantify three-dimensional current fields at tidal inlets, navigational channels, and in other shallow marine and estuarine environments. Table 2 summarizes deployment configurations that are applicable to coastal engineering surveys in relatively shallow water.

Figure 11 illustrates the moving deployment configuration on a small coastal vessel. In this case, the ADCP can be interfaced with navigation software and accounts for the vessel motion by tracing the bottom. An ADCP sensor can also be deployed on a taught line mooring as shown in Fig. 12. Bottom mount configurations often use trawl-resistant moorings as shown in Fig. 13.

Fig. 11. Side-mounted ADCP sensor for moving deployment application (photo from the US Geological Survey).

Figure 14 shows a time series of ADCP data collected from a shallow estuary using a bottom-mounted configuration. The grayscale plot (originally in color) indicates the intensity of the velocity in the along-estuary direction with respect to depth (Zarillo, 2002). The lower panel shows the vertically averaged velocity and clearly shows the current speed and direction changing at the semidiurnal tidal frequency dominant in the estuary. Since ADCP technolgy and be used to collect current data over a vertical profile or even along an horizontal profile across a channel or inlet throat, it is possible to apply ADCP data to calibrate three-dimensional hydrodynamic models. For example, Fig. 15 compares ADCP derived velocity in six vertical bins with predicted velocity in 5-vertical layers of a numerical circulation model in a shallow estuary.

2.7.3. *Nearshore directional wave measurements*

The measurement of wave energy, and in particular, directional spectra, has been one of the more difficult problems in observational coastal engineering. ADCPs combine the required functionality to measure both waves and currents in relatively shallow

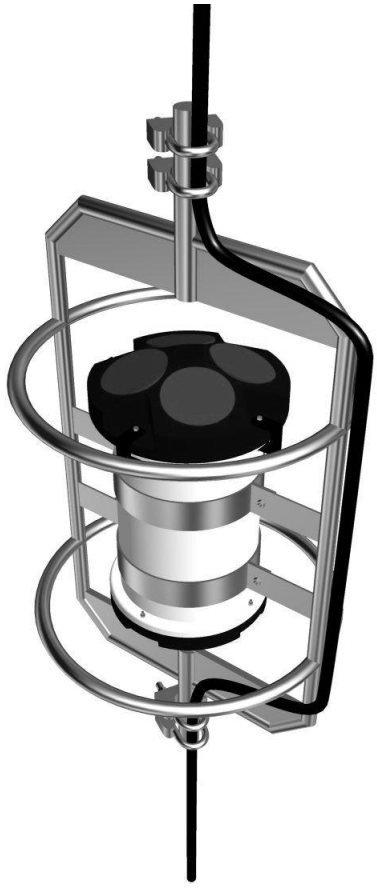

Fig. 12. Example of a taught line ADCP mount for mid-depth deployment.

Fig. 13. ADCP trawl resistant bottom mount.

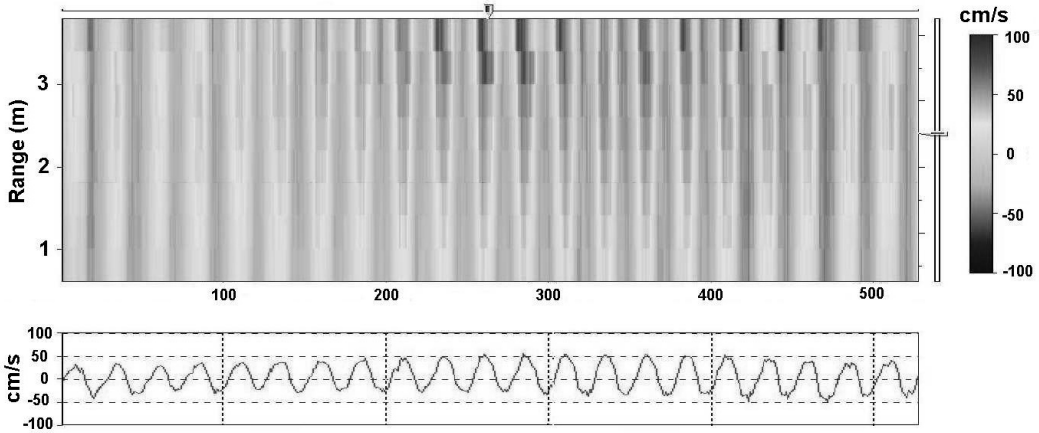

Fig. 14. Top panel: ADCP record showing the vertical distribution of velocity over 5 bins. Bottom panel: Depth average velocity across 5 bins. Positive values indicate north-directed flow and negative values indicate south-directed flow.

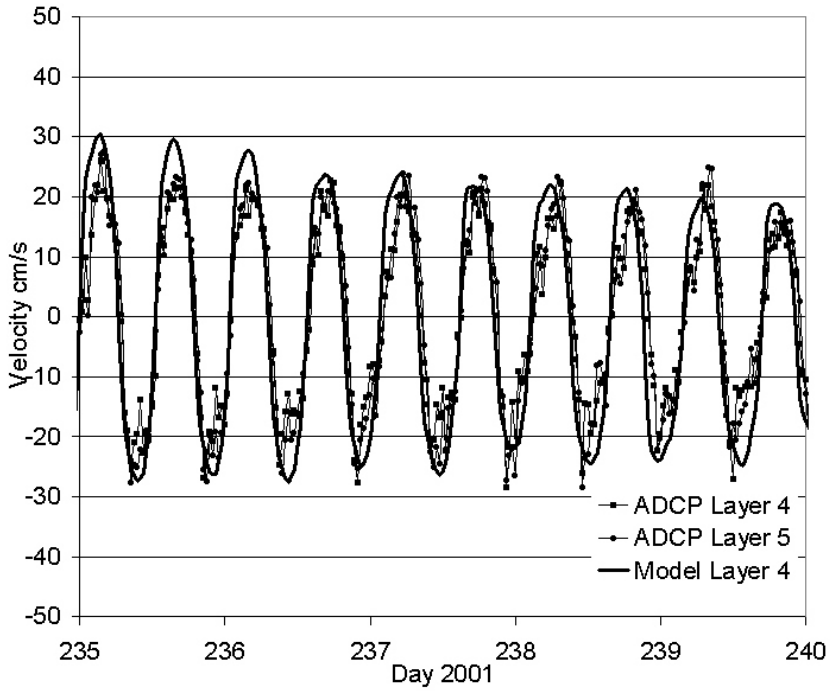

Fig. 15. Comparison of measured velocity from near surface ADCP bins with velocity predicted in a near surface layer of a three-dimensional hydrodynamic model of a shallow estuary (Zarillo, 2002).

water and therefore there has been considerable interest in exploring their capabilities for measuring wave spectra. The work of Pinkel and Smith (1987) and Krogstad *et al.* (1988) demonstrated that a Doppler sonar using horizontally projected beams could provide a high quality measurement of wave direction. Whereas, these early contributions made advancements on various aspects of the problem, they were not comprehensive, and contained little comparison data to assess the performance of the ADCP against commonly used wave direction sensors, such as heave-pitch-roll buoys and pressure velocity (PUV) type sensors.

Recently, Strong *et al.* (2000) reported on the advancements in ADCP technology for directional wave measurements and presented comparisons with more conventional wave gauges. In ADCP wave measurements the range cells along the acoustic beams constitutes a sparse array of independent sensors that measures the local instantaneous velocity projected along the beam. The auto- and cross-spectra of these signals in each frequency band are assumed to be known linear functionals of the directional distribution of the waves. Wave direction can be estimated by inverting this "forward" relation using the Iterative Maximum Likelihood Method (Krogstad *et al.*, 1988; Terray *et al.*, 1990). The elements of the cross-spectral matrix at any frequency (or wavenumber) contain directional information in both their phase and amplitude. Thus, the ADCP lies partway between a pure array measurement, relying solely on phase, and a point sensor such as a PUV gauge. Figure 16 compares surface wave spectra derived from an InterOcean S4^{tm} sensor with an RDI^{tm} 1200 kHz ADCP unit. The S4 acquires directional wave information using the standard PUV configuration collecting pressure and velocity data at sampling rate of 2 Hz (Rørbæk and Andersen, 1997). It can be seen that the surface elevation results from the S4 and ADCP unit are nearly identical.

Figure 17 compares the directional energy distribution calculated from the S4 and ADCP sensors. The comparison shows that the Maximum Entropy Method (MEM) of analysis used to extract directional data from the S4 measurements yields a broader and smoother directional distribution compared with the Maximum Likelihood Method (MLM) analysis of the ADCP measurements. Other comparisons yielded similar results and indicate that the MEM consistently resolves directional seas somewhat better than the MLM for both unimodal as well as bimodal seas (Nwogu *et al.*, 1987). However, Rørbæk and Andersen (1997) noted that both methods require that the wave field is spatially homogeneous, hence effects from diffraction, refraction, and reflection may influence on the results (due to phase locking). Under these conditions, Nwogu, *et al.* (1987) suggest that both methods become inaccurate with the MLM being the least accurate.

2.8. *Geographical information system methods*

Aerial photography in digital format is commonly analyzed to study the evolution of coastal systems. Standard aerial photography is generally of high geometric fidelity

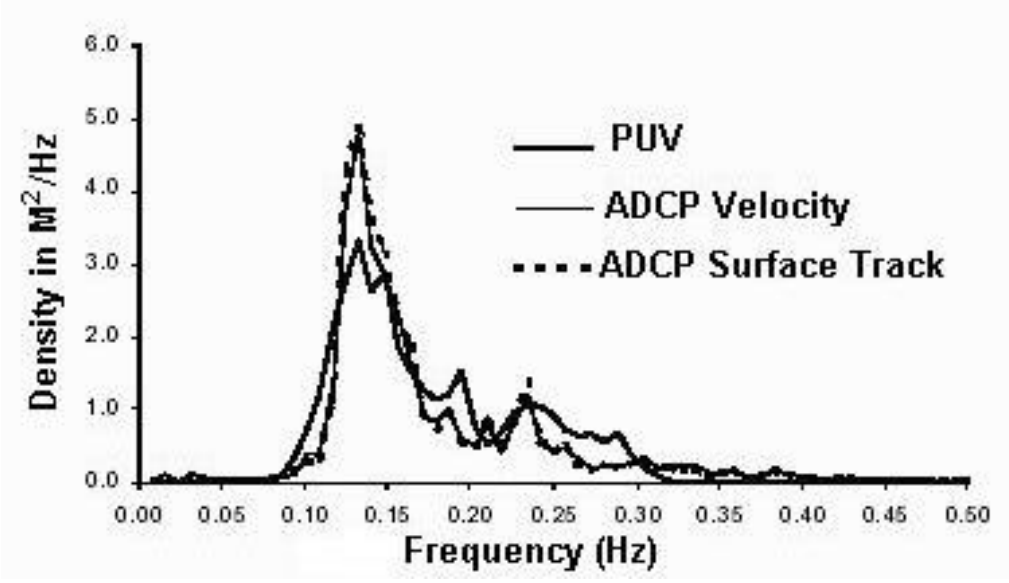

Fig. 16. Comparison of energy distribution acquired by PUV and ADCP type wave gauges (adapted from Rørbæk and Andersen, 1997).

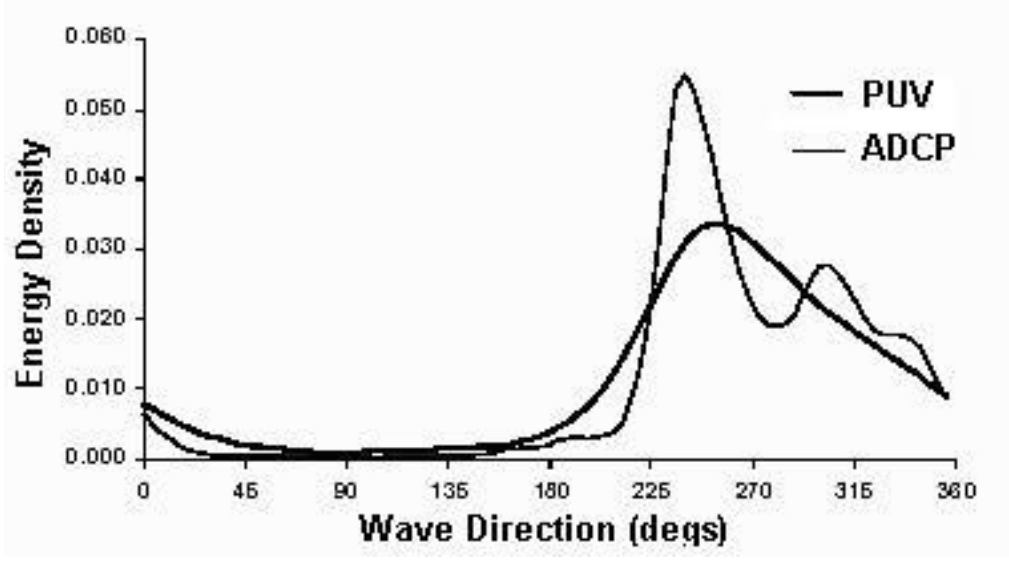

Fig. 17. Relative energy as a function of the wave direction derived from a PUV type sensor and an RDI 1200 kHz ADCP unit (adapted from Rørbæk and Andersen, 1997).

and very useful in the coastal regions of moderate to low topographic relief. Accurate measurements of shoreline position, dune vegetation, and overall geomorphic change can be made and compared over time when adequate temporal and spatial coverage is available. Methodology for calculating sediment budgets, analyzing inlet

shoal volumes, measuring coastal change using data derived from aerial photography can be found in widely available coastal engineering publications (Rosati and Kraus, 1999). However, despite the widespread use of aerial photography and associated photogrammetric methods in coastal studies, image analysis methods to more efficiently and automatically extract data from digital imagery have not been in widespread use by the coastal engineering community. Image analysis methods commonly applied for land use studies, oceanographic data collection and meteorological monitoring can be adapted to improve data collection and analysis for coastal engineering.

Traditional remote sensing methods involve examination of the spectral signature of remote sensing data using image analysis techniques. The principles of remote sensing and image analysis can be found in textbooks such as the Manual of Remote Sensing (American Society of Photogrammetry, 1983), Remote Sensing and Image Interpretation (Lillesand and Kiefer, 1994), Introductory Digital Image Processing (Jensen, 1996), and many others. The major categories of image analysis include digital filtering, image registration, image enhancement, and image classification. To date image registration has been the most frequently used image processing methods in general use for coastal engineering studies. An example is the digital orthographic quarter quadrangle (DOQQ) aerial imagery that has been freely distributed by the US Geological Survey (USGS). These digital images have been widely applied by coastal zone managers to provide base maps for developing land use themes in GIS format. Digital handling of the image raster data using data decimation schemes allows desktop viewing and manipulation of large image files having a spatial resolution as fine as 1 m without compromising computational effort.

GIS technology was developed as an extension to traditional mapping methods once computing technology advanced to a point of rapid calculations. Similar to remote sensing technology, GIS methods have only been slowly adopted as a tool in coastal engineering. Recent improvements in computer software and hardware have allowed both remote sensing and GIS to assume a major role in the managements of coastal resources. State and Federal agencies in the United States use GIS technology to archive and disseminate data critical for coastal zone management. As an example, the NOAA Coastal Services Center in Charleston, SC is a clearinghouse for spatial data relating to the management of coastal environments. Among the data sets that are available in GIS are vectorized shoreline data, land use themes for United States coastal regions, benthos habitat data, and coastal change data. Many of these data sets combine remote sensing data and GIS methods for convenient display.

The essentials of GIS methods can be found in textbooks such as *Fundamentals of Geographic Information Systems* (Demers, 1996). The improving speed and mass storage of desktop computing during the 1990s provided an opportunity to combine remote sensing and GIS methods into a single desktop platform. An example is the adaptation of the USACE SBAS software to the ArcView^{TM} GIS platform (Rosati and Krau, 1999). This software package combines aspects of remote sensing

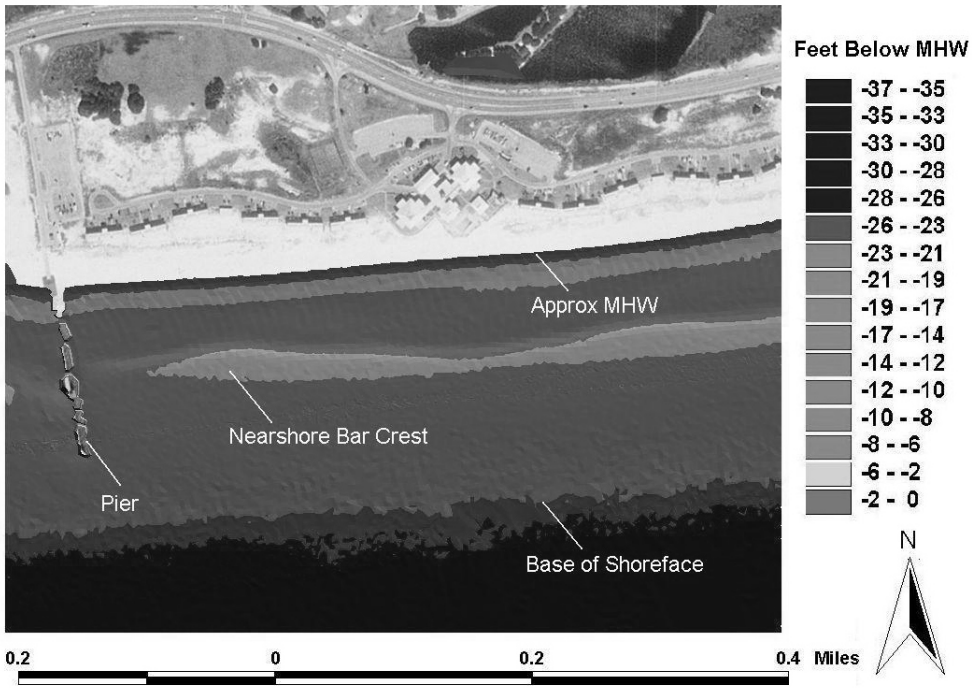

Fig. 18. GIS presentation of LIDAR data showing the details of the shore face at Gulf Shores State Park, Alabama. LIDAR data are superimposed on USGS digital ortho imagery.

and GIS to provide a tool for calculating shoreline sediment budgets. Another example of combined remote sensing and GIS methods in coastal engineering is a toolbox for handling large arrays of LIDAR data in a customized GIS platform. The SHOALS Toolbox (Wozencraft *et al.*, 2002) allows relatively automated manipulation and plotting of LIDAR-based topographic data collected from beach and nearshore zones. Figure 18 is an example of a GIS presentation of LIDAR data superimposed on a USGS DOQQ image of Gulf Shores State Park in Alabama, USA. The 4-m spatial resolution of the LIDAR data allows the details of the near shore bar system and coastal structures to be easily identified.

2.9. *Image analysis methods*

The aerial photographic record for many coastal regions extends back to the 1940s and even earlier for some locations. Such documentation often contains information about coastal morphology prior to major engineering projects. This is particularly true for tidal inlets since historical photographs can provide quantitative data on coastal morphology pre- and post-jetty construction. Photographs thus contain substantial information about the response of the inlet and nearshore morphology to navigation channel operation and maintenance activities. An additional advantage is that historical aerial photographs can usually be obtained at a relatively low cost

from government agencies or private aerial surveying firms that maintain archives of their photography. Very often more than a century of coastal change can be represented using a combination of historical maps and aerial photographs. Using GIS as a common platform, it is possible to reduce maps in digital form and digital aerial photos to a common geographic datum.

Since digital imagery can be easily imported to most GIS platforms and georeferenced to base maps or other images (i.e. USGS DOQQ's) the next logical step is to apply image analysis methods for enhancing the utility of coastal aerial photography. Recent developments in this area include extensions to GIS software that combine the power of image analysis with the convenient manipulation of geographic data. Image analysis methods that have been applied to accomplish this include relatively simple image enhancement and image classification techniques. Hoeke and Zarillo (2001) described an extension to ArcView™ 3.× that allows automated mapping of the shoreline and vegetation lines along the coast. Similarly, Connell and Zarillo (2003) extended the method to include automated mapping of inlet channels and shoals. The most important feature of these tools is the ability to reduce all data to a common horizontal datum, compare data sets over time, and automate extraction digital data for time series analysis. Thus, the image analysis method allows data acquisition using a spectral signature, whereas the GIS aspect of the methodology allows comparison of temporal change in a common geographic reference system.

Hoeke and Zarillo (2001) demonstrated how image analysis methods can be applied to automate mapping of important coastal features using simple image analysis within a GIS platform. The Beachtools GIS extension (Hoeke and Zarillo, 2001) developed as a tool for studying historical shoreline change from aerial photography; specifically, to automatically map the wet/dry line and the vegetation line of the beach (Fig. 19), and generate transects from a standardized baseline to these features. The Beachtools extension was coupled with the ArcView™ 3.×, since this widely used GIS platform already included a powerful image analysis extension termed ImageAnalyst. The inclusion of vegetation line measurements is considered an important indicator of shoreline position, as well as the wet/dry line, which approximates the position of mean high water (Smith and Zarillo, 1990). The vegetation line provides an estimate of the position of the toe of the dune and is a less variable indicator of long-term shoreline change since the response of the vegetation line to erosion or accretion is on the order of months to years, rather than the higher frequency changes of the wet/dry lines.

The Beachtools GIS extension is based on a supervised spectral classification of the highly reflective beach sand with respect to the surrounding wet or saturated areas below the high water line and vegetated zone. Similar to a supervised classification for extracting land cover thematic information, a group of image picture elements (pixels) representing the reflective beach are selected as a training site (Jensen, 1996). The statistics of the spectral reflectance within the training site are used to identify all other pixels in the digital image having similar reflectance

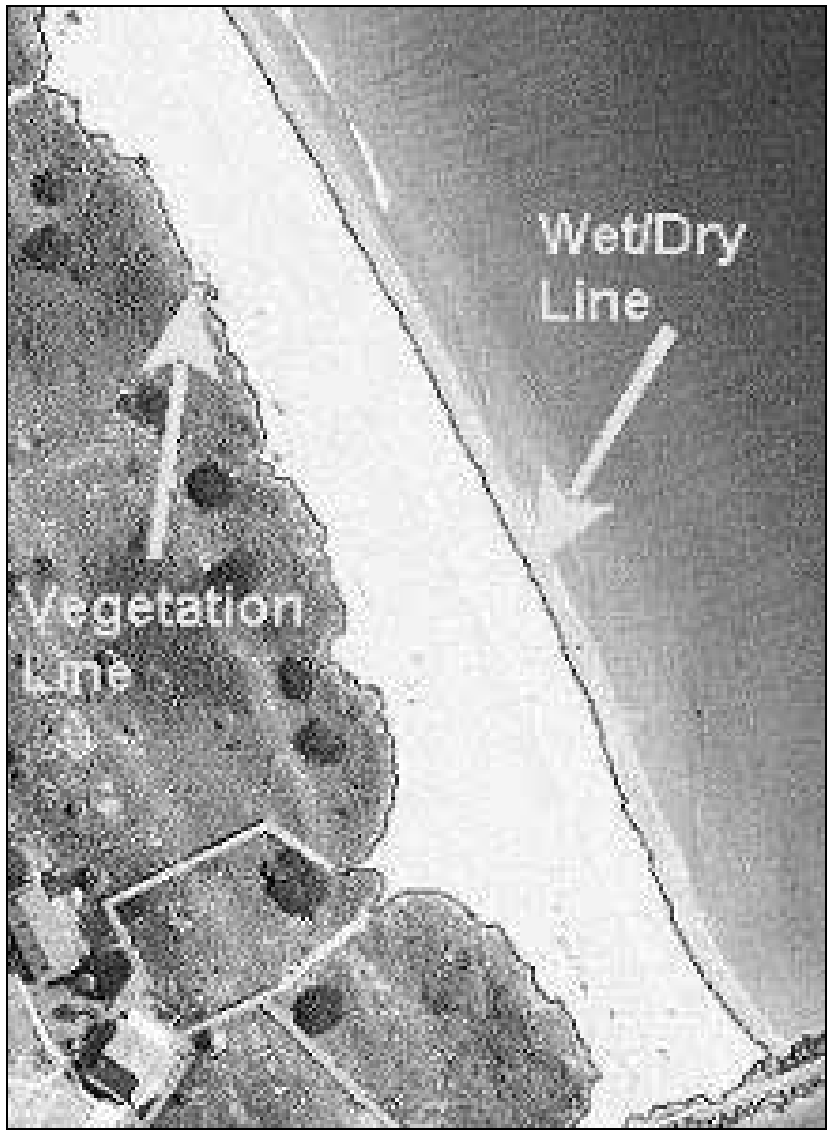

Fig. 19. Shoreline and vegetation line extracted from digital aerial photography using supervised image classification methods (BeachTools).

values in the visible portion of the spectrum. The capabilities of the combined image analysis and GIS approach to shoreline mapping GIS include:

(a) Image rectification against a georeferenced base map or ortho-imagery.
(b) Image histogram stretching (image enhancement for contrast).
(c) Automatic delineation of coastal features using spectral classification.
(d) Baseline and transect generation tools.
(e) Generation of data files containing measurements of shoreline position.

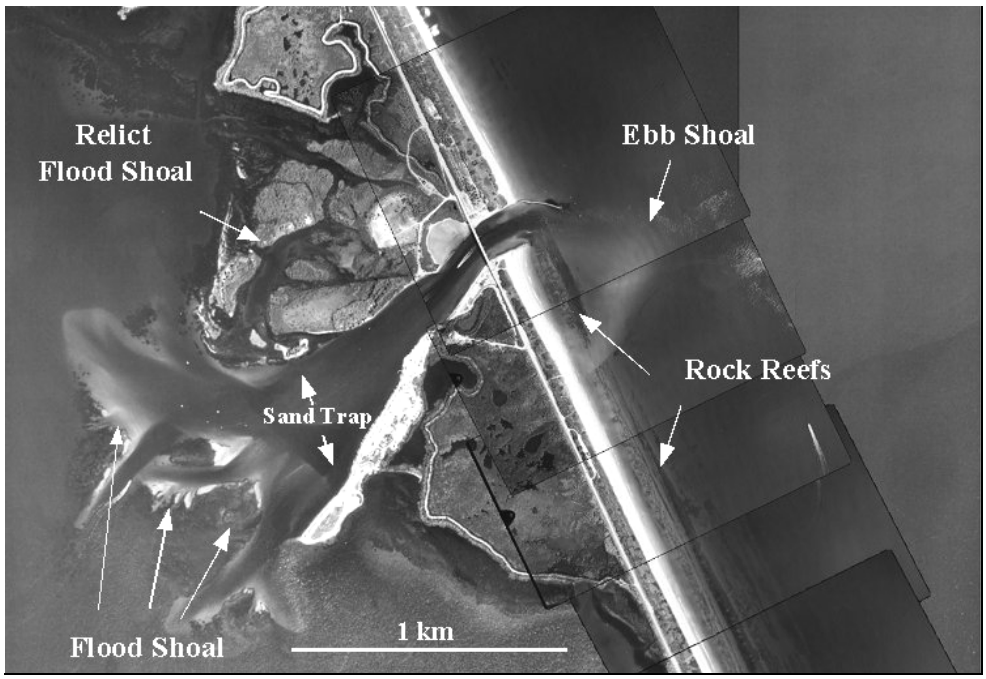

Fig. 20. Photo mosaic of the central Florida Sebastian Inlet area created by rectifying to a USGS digital ortho-image using the ArcView^{TM}. Beachtools GIS extension.

Figure 20 is a photo mosaic of the central Florida coast in the vicinity of Sebastian Inlet created by rectifying digitized aerial photography against a regional ortho-image database. Figure 21 shows the details of the vegetation line and shoreline extracted within the GIS platform using image analysis methods. Also shown are a series of cross-shore transects automatically placed along the shoreline at a user specified interval, allowing quantification of shoreline position. Figure 22 illustrates the possibility of a power spectrum analysis using the high-resolution data extraction that is available using the capabilities of GIS.

Image analysis of common aerial photography has also been under-utilized in examining tidal inlet dynamics. The INLETGIS extension to ArcView^{TM} 3.$\times$ was developed to automate many of the steps involved in shoal and channel change analysis using aerial imagery (Connell and Zarillo, 2003). The result is a tool that facilitates rapid data turn-around, less subjectivity, and a gentle learning curve, thus serving users with a broad range of scientific and engineering backgrounds in need of a rapid, objective image analysis tool.

Inlet morphology classification can be based on spectral reflectance pattern recognition. For example, the classification shown in Fig. 23 was applied to the water and shoal portions of a digital historical photoset of a tidal inlets to determine where

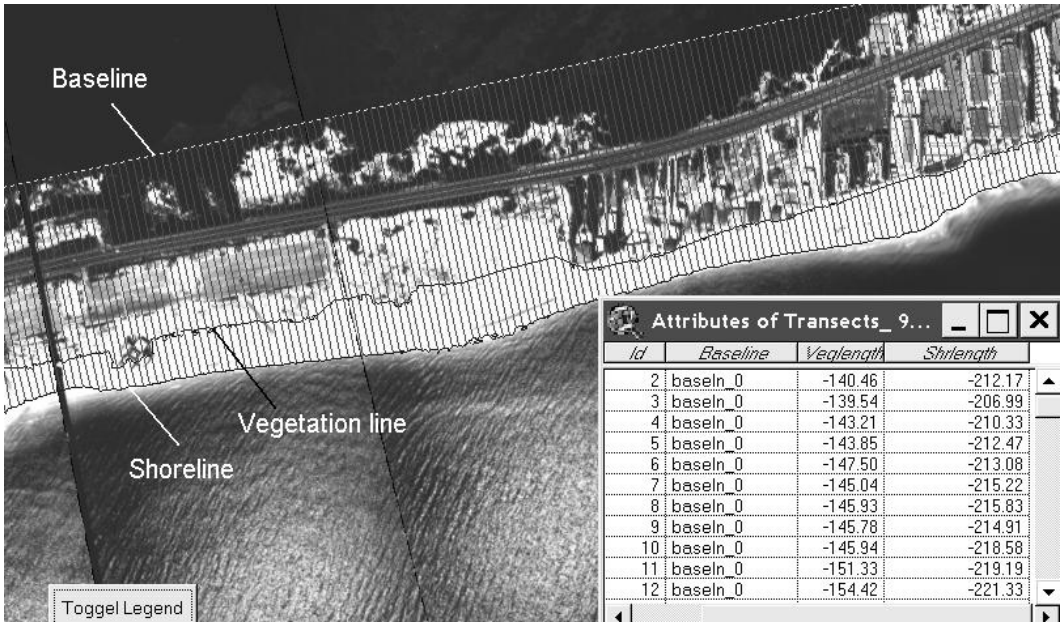

Id	Baseline	Veglength	Shrlength
2	baseln_0	-140.46	-212.17
3	baseln_0	-139.54	-206.99
4	baseln_0	-143.21	-210.33
5	baseln_0	-143.85	-212.47
6	baseln_0	-147.50	-213.08
7	baseln_0	-145.04	-215.22
8	baseln_0	-145.93	-215.83
9	baseln_0	-145.78	-214.91
10	baseln_0	-145.94	-218.58
11	baseln_0	-151.33	-219.19
12	baseln_0	-154.42	-221.33

Fig. 21. Example of high resolution shoreline mapping in GIS. Vegetation and wet/dry lines were mapped using image analysis. Table insert shows the automated extraction of shoreline position with respect to a baseline.

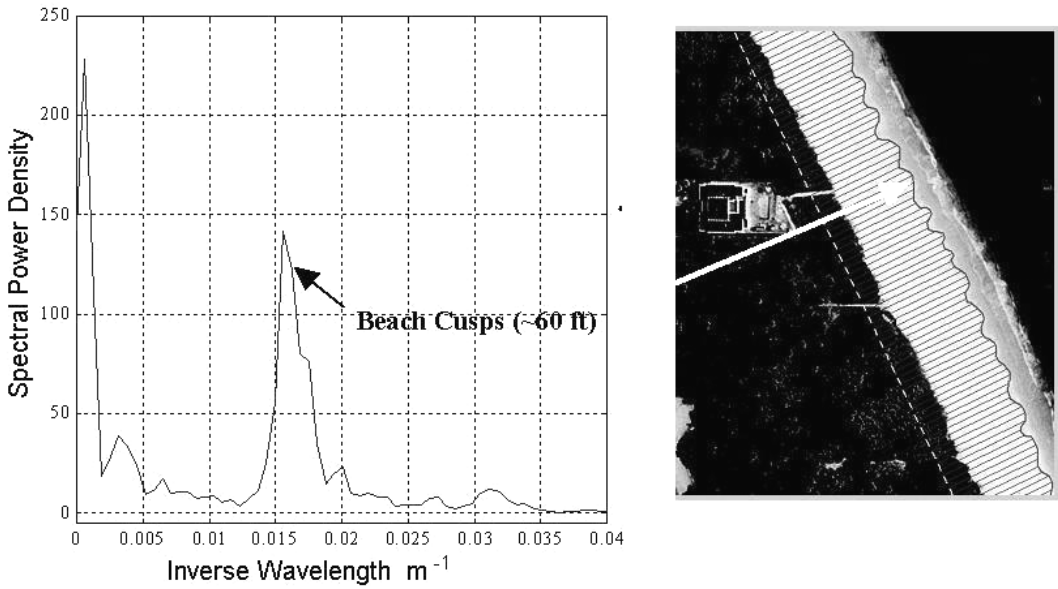

Fig. 22. Example of high resolution shoreline mapping used to compute power spectrum of cuspate beach morphology.

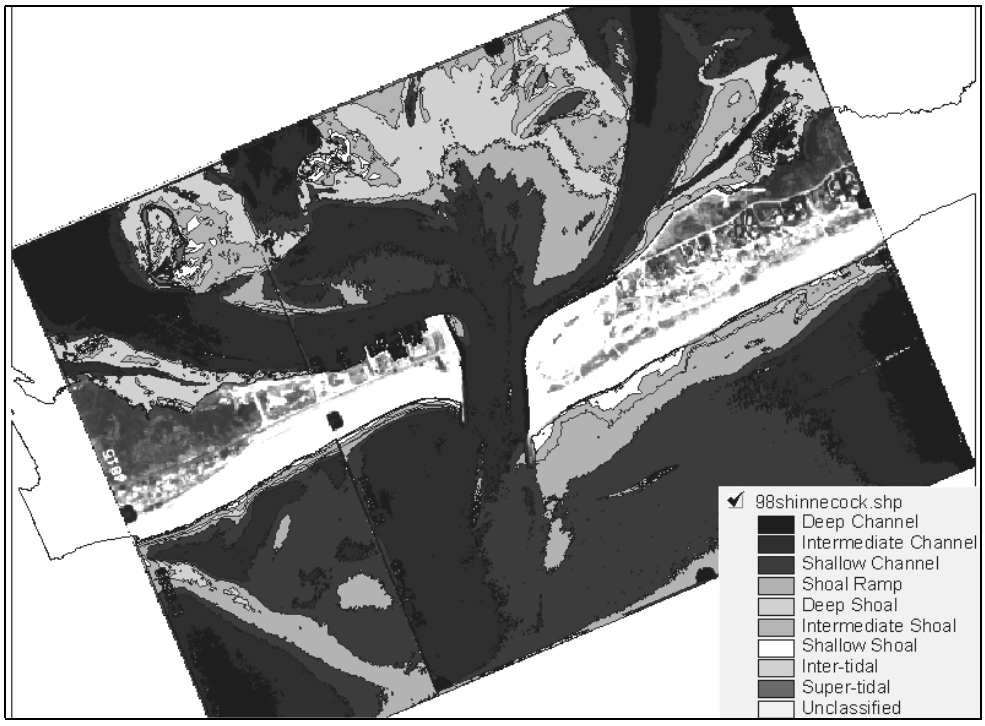

Fig. 23. Identification of tidal inlet morphology using the supervised image classification method.

channels, sub-tidal shoals, inter-tidal shoals, and super-tidal shoals spatially occur in the image. Once a classification scheme is created, temporal pattern recognition from one photograph or photo mosaic the next in a time sequence can be analyzed to determine changes in channel behavior and shoaling.

The examples of image analysis and remote sensing methods provided in the previous sections largely involve the use of visible and near infrared panchromatic digital imagery obtained from fixed wing low altitude aircraft, i.e. common aerial photography.

The merging of satellite remote sensing and GIS technology have produced a wide array of application for mapping coastal habitats, and detecting change in terms of vegetation, sediment type, and water quality. Satellite based remote sensing methods commonly used for environmental analysis can provide an alternative to the use of aerial photography for coastal analysis. The temporal resolution of near polar orbiting satellites can improve the coverage of the costal zone that is required to map and quantify the abrupt and rapid changes that characterize coastal morphology. However, until recently the spatial resolution of satellite imagery did not allow detailed geomorphic analysis required for engineering work. Satellite imagery in the visible and near infrared portions of the spectrum is now available at a spatial resolution competitive with digital aerial images. Table 3 summarized the

Table 3. Typical spectral features of high-resolution commercial satellite imagery.

Spectral Region	Spectral Range in Microns	Image Spatial Resolution
Panchromatic	0.45–0.90	1 meter
Band 1 (blue)	0.45–0.52	Approximately
Band 2 (green)	0.51–0.60	4-meter
Band 3 (red)	0.63–0.70	multispectral
Band 4 (near IR)	0.76–0.85	

major features of commercially available satellite imagery in the optical part of the spectrum where remote sensing data can be applied to coastal studies. The repeat cycle for a particular geographic location depends on the latitude, but generally the mid-latitudes are revisited every 3 to 8 days.

Generally commercial satellite imagery can be acquired in GIS-ready format including georeferencing to either local or UTM coordinate systems. The spatial resolution in the panchromatic band is on the order of 1 meter, whereas the resolution in 4-band multispectral images is on the order of 4 meters (Table 3). Although the excellent temporal and spatial resolution of currently available commercial satellite data would facilitate application to shoreline change and geomorphic analysis this application is still under development. Due to relatively low cost and high temporal resolution satellite imagery may eventually replace aerial photography as the main tool for coastal change analysis.

Among the many possible uses of satellite remote imagery, bathymetric data acquisition holds promise for having a significant advantage in cost and resolution in coastal regions having relatively clear water. Algorithms for extracting depth from multispectral imagery have already been tested to a limited extent (Lyzenga, 1978; Stumpf and Holderied, 2003).

Standard algorithms for determining depth in clear water from passive multispectral remote sensors where sensors already exist, but require several tuning parameters (Stumpf and Holderied, 2003). In additional, existing algorithms have difficulty in retrieving depths where the bottom has an extremely low albedo. In ongoing work to develop practical depth extraction from shallow marine environments, empirical solutions, having fewer tunable parameters, could be applied to a larger range of albedo features using spectral reflectance bands of high resolution satellite imagery. The two algorithms, a standard linear transform, and a ratio transform will be compared using IKONOS satellite imagery and LIDAR bathymetry from Palm Beach County, Florida. Stumpf and Holderied (2003) used this approach for extracting depth in shallow coral reef environments. To date, however spectral remote sensing methods for depth extraction have not been adapted to coastal zones having sediment constructed beach and nearshore profiles. In the near future, however, algorithms based on combinations of three visible and one infrared band of the

satellite imagery are expected to be able to compensate for variable bottom type and albedo, including mixtures of sand and rock outcrops. Tuning of multispectral depth algorithms can be accomplished by comparison to the LIDAR surveys. Given the spatial resolution multispectral imagery is approximately 4 m and it is expected that the overall accuracy and resolution of spectral-based depths extraction will be comparable to LIDAR survey methods, but at a small fraction of the cost.

3. Summary

Tidal inlets and tidal waterways serve as the entrance channel to many harbors and shipping ports throughout the world. This is certainly true for the East and Gulf Coasts of the United States where barrier chains and tidal inlets form much of the coast. Many of world's tidal inlets are dredged on a regular basis and many others will be modified with engineering structures. USACE is responsible for maintaining 12,000 miles of navigable waterways and in 2001, the federal government spent $867.7 million to maintain its navigation channels (USACE, 2003). Potential savings in channel maintenance costs and in the development of engineering plans are dependent on efficient collection, analysis, and interpretation of wave, tide, sedimentologic, and morphologic data. As described in this paper these needs are being met with new equipment, new approaches to tidal inlet research using existing technology, and innovative means of analyses.

Acknowledgements

The authors of this paper appreciate the financial and technical support provided by the Coastal Inlets Research Program, USACE. Permission was granted by Headquarters, US Army Corps of Engineers, to publish this information.

References

Abraham, D. and Pratt, T. (2002). Quantification of bed-load transport using multibeam survey data and traditional methods, ERDC/CHL CHETN-VII-4, US Army Engineer Research and Development Center, Vicksburg, MS.

American Society of Photogrammetry (1983). *Manual of Remote Sensing*, 2nd edn. Editor-in-Chief R. N. Colwell, Falls Church, VA, 2 volumes, 2440 pp.

Blair, J. B., Rabine, D. L. and Hofton, M. A. (1999). The laser vegetation imaging sensor: A multi-altitude, digitization-only, airborne laser altimeter for mapping vegetation and topography, *ISPRS Journal of Photogrammetry and Remote Sensing* **54**: 115–122.

Bolivar, L., Carter, W. and Shrestha, R. (1995). Airborne laser swath mapping aids in assessing storm damage, *Florida Engineering*, pp. 26–27.

Boon, J. D., III and Byrne, R. J. (1981). On basin hypsometry and the morphodynamic response of coastal inlet systems, *Marine Geology* **40**: 27–48.

Boothroyd, J. C. and Hubbard, D. K. (1975). Genesis of bedforms in mesotidal estuaries, ed. L. E. Cronin, *Estuarine Research* **2** (Academic Press, New York) 217–235.

Brock, J. and Sallenger, A. (2001). Airborne topographic lidar mapping for coastal science and resource management, US Geological Survey Open-File Report 01–46.

Bruun, P. and Gerritsen, F. (1959). Natural bypassing of sand at coastal inlets, *Journal of Waterways and Harbors Division* **85**: 75–107.

Buonaiuto, F. S. and Kraus, N. C. (2003). Limiting slopes and depths at ebb-tidal shoals, *Coastal Engineering* **48**: 51–65.

Buynevich, I. V., Evans, R. L. and FitzGerald, D. M. (2003). High-resolution geophysical imaging of buried inlet channels, *American Society of Civil Engineers*, Coastal Sediments 2003 Proceedings, 15 pp.

Buynevich, I. V., FitzGerald, D. M. and Parolski, K. F. (1999). Geophysical investigation of the nearshore geologic framework, Eastern Casco Bay — Reid State Park, Maine: Data interpretation and mplications for Late Quaternary coastal evolution, US Geological Survey Open-File Report 99–0380, 32 pp.

Buynevich, I. V., FitzGerald, D. M., Smith. L. B., Jr. and Dougherty, A. J. (2001). Stratigraphic evidence for the historical position of the East Cambridge shoreline, Boston Harbor, Massachusetts, *Journal of Coastal Research* **17**: 620–624.

Connell, K. and Zarillo, G. A. (submitted). Tidal Inlet Shoal and Channel Change Analysis from Aerial Imagery Using Inlet, Nearshore, and Littoral Enhancement Tool for Geographic Information Systems (INLETGIS). Coastal and Hydraulics Engineering Technical Note IV-xx, US Army Engineer Research and Development Center, Vicksburg, MS, 14 pp.

Costa, S. L. and Glatzel, K. A. (2002). Humboldt Bay, California, Entrance Channel, Report 1: Data Review. ERDC/CHL TR-02-1, US Army Engineer Research and Development Center, Vicksburg, MS.

Dalrymple, R. W., Knight, R. L. and Lambias, J. J. (1978). Bedforms and their hydraulic stability relationships in a tidal environment, Bay of Fundy, Canada, *Nature* **275**: 100–104.

DeAlteris, J. A. and Byrne, R. J. (1975). The recent history of Wachapreague Inlet, Virginia, ed. L. E. Cronin, *Estuarine Research*, Academic Press, New York, **2**, pp. 167–181.

Demers, N. N. (1996). *Fundamentals of Geographic Information Systems*, John Wiley & Sons, 504 pp.

Dronkers, J. J. (1964). *Tidal Computations in Rivers and Coastal Waters* North Holland, Amsterdam, 518 pp.

Fenster, M. S. and FitzGerald, D. M. (1996). Morphodynamics, stratigraphy, and sediment transport patterns of the Kennebec River estuary, Maine, USA, *Sedimentary Geology* **100**: 123–145.

Fenster, M. S., FitzGerald, D. M., Bohlen, W. F., Lewis, R. S. and Baldwin, C. T. (1990). Stability of giant sand waves in Eastern Long Island Sound, *Marine Geology* **91**: 207–225.

FitzGerald, D. M., Buynevich, I. V., Davis Jr., R. A. and Fenster, M. S. (2002). New England tidal inlets with special reference to rivering-associated inlet systems, *Geomorphology* **48**: 179–208.

FitzGerald, D. M. and Pendleton, E. (2002). Inlet formation and evolution of the sediment bypassing system: New inlet, Cape Cod, Massachusetts, *Journal of Coastal Research* **36**: 290–299.

FitzGerald, D. M., Kraus, N. C. and Hands, E. B. (2001). Natural mechanisms of sediment bypassing at tidal inlets, ERDC/CHL-IV-A, US Army Engineer Research and Development Center, Vicksburg, MS. (http://chl.wes.army.mil/library/publications/cetn), 11 pp.

FitzGerald, D. M., Buynevich, I. V., Fenster, M. S. and McKinlay, P. A. (2000). Sand dynamics at the mouth of a rock-bound, tide-dominated estuary, *Sedimentary Geology* **131**: 9–25.

FitzGerald, D. M. (1996). Geomorphic variability and morphologic and sedimentologic controls on tidal inlets, *Journal of Coastal Research* **SI 23**: 47–71.

FitzGerald, D. M., Rosen, P. S. and van Heteren, S. (1994). New England Barriers, ed. R. A. Davis, *Geology of Holocene Barrier Island Systems*, Springer-Verlag, Berlin, Chap. 8, pp. 305–394.

FitzGerald, D. M. and Montello, T. M. (1993). Backbarrier and inlet sediment response to the breaching of Nauset Spit and formation of New Inlet, Cape Cod, MA, eds. D. G. Aubrey and G. S. Giese, *Formation and Evolution of Multiple Tidal Inlet Systems* (AGI) 158–185.

FitzGerald, D. M. (1988). Shoreline erosional-depositional processes associated with tidal inlets, eds. D. G. Aubrey and L. Weishar, *Hydrodynamics and Sediment Dynamics of Tidal Inlets*, Springer-Verlag, New York, 269–283 pp.

FitzGerald, D. M. and Nummedal, D. (1983). Response characteristic of an ebb-dominated inlet channel, *Journal of Sediment Petrology* **53**: 833–845.

FitzGerald, D. M. and FitzGerald, S. A. (1977). Factors influencing tidal inlet throat geometry, *Proc. Coastal Sediments '77, American Society of Civil Engineers*, pp. 563–581.

FitzGerald, D. M. and Nummedal, D. (1977). Ebb-tidal delta stratification, ed. D. Nummedal, *Beaches and Barriers of the Central South Carolina Coast Fieldtrip Guidebook for Coastal Zone*, 1977, Coastal Engineering Conference, pp. 39–44.

Fry, V. A. and Aubrey, D. G. (1990). Tidal velocity asymmetry and bedload transport in shallow embayments, Estuarine, Coastal, and Shelf Science, **30**: 453–473.

Gibeaut, J. C. and Davis, R. A. (1993). Statistical geomorphic classification of ebb-tidal deltas along the west central Florida coast, *Journal of Coastal Research* **SI 118**: 165–184.

Hine, A. (1975). Bedform distribution and migration patterns on tidal deltas in the Chatham Harbor Estuary, Cape Cod, Massachusetts, ed L. E. Cronin, Estuarine Research, Academic Press, New York, **2** 217–235 pp.

Hoeke, R. C. and Zarillo, G. A. (2001). A GIS-based tool for extracting shoreline positions from aerial imagery, Coastal and Hydraulics Engineering Tec0, Coastal and Hydraulics Laboratory, Vicksburg, MS, 12 pp.

Hubbard, D. K. (1975). Morphology and hydrodynamics of the Merrimack River ebb-tidal delta, ed. L. E. Cronin, *Estuarine Research* Academic Press, New York, **2**, pp. 253–266.

Irish, J. L. and Lillycrop, W. J. (1997). Monitoring New Pass, Florida, with high density lidar bathymetry, *Journal of Coastal Research* **13**: 1130–1140.

Irish, J. L. and Lillycrop, W. J. (1999). Scanning laser mapping of the coastal zone: The SHOALS system, *ISPRS Journal of Photogrammetry & Remove Sensing* **54**: 123–129.

Jarrett, J. T. (1976). Tidal prism-inlet area relationships, GITI Report 3. US Army Engineer Waterways Experiment Station, Vicksburg, MS.

Jensen, J. R. (1996). *Introductory Digital Image Processing*, Prentice Hall, Upper Saddle River, NJ 316 pp.

Jol, H. M., Smith, D. G. and Meyers, R. A. (1996). Digital ground penetrating radar (GPR): An improved and very effective geophysical tool for studying modern coastal barriers (examples for the Atlantic, Gulf and Pacific coasts, USA), *Journal of Coastal Research* **12**: 960–968.

Kraus, N. C. (2000). Reservoir model of ebb-tidal shoal evolution and sand bypassing, *Journal of Waterway, Port, Coastal, and Ocean Engeering* **126**: 305–313.

Kraus, N. C., Zarillo, G. A. and Tavolaro, J. F. (2003). Hypothetical relocation of Fire Island Inlet, New York, *American Society of Civil Engineers, Coastal Sediments 2003 Proceedings*, 14 pp.

Kraus, N. C. (1998). Inlet cross sectional area calculated by process-based model, *Proc. 26th Coastal Eng. Conf.*, American Society of Civil Engineers **3**: 265–278.

Krabill, W. B., Wright, C. W., Swift, R. N., Frederick, E. B., Manizade, S. S., Yungel, J. K., Martin, C. F., Sonntag, J. G., Duffy, M., Hulslander, W. and Brock, J. C. (2000). Airborne laser mapping of Assateague National Seashore Beach, Photogrammetric Engineering & Remote Sensing **66**: 65–71.

Krogstad, H. E., Gordon, R. L. and Miller, M. C. (1988). High resolution directional wave spectra from horizontally-mounted acoustic Doppler current meters, *Journal Atmospheric and Oceanic Technology* **5**: 340–352.

LeConte, L. J. (1905). Discussions of "Notes on the improvement of rivers and harbor outlets in the United States" by P. A. Watts, *Transactions of American Society of Civil Engineers* **55**: 306–308.

Lillisand, T. M. and Keifer, R. W. (1994). *Remote Sensing and Image Interpretation*, 3rd edn. (John Wiley & Sons) 750 pp.

Lyzenga, D. R. (1978). Passive remote sensing techniques for mapping water depth and bottom features, *Appl. Opt.* **17**: 379–383.

McClung, J. K. and Douglass, S. L. (1999). Observing changes in an ebb-tidal shoal, Coastal sediments '99, eds. N. C. Kraus and W. G. McDougal, *4th International Symposium on*

Coastal Engineering and Science of Coastal Sediment Processes; Scales of Coastal Sediment Motion and Geomorphic Change, Hauppauge, New York, United States, pp. 734–749.

Mitchum, R. M., Jr., Vail, P. R. and Sangree, J. B. (1977). Stratigraphic interpretation of seismic reflection patterns in depositional sequences, ed. C. E. Payton, *Seismic Stratigraphy — Application to Hydrocarbon Exploration*, American Association of Petroleum Geologists Memoirs **26**: 117–133.

Mohr, M. C., Pope, J. and McClung, J. K. (1999). Coastal response to a detached breakwater system, Presque Isle, Erie, PA, USA Coastal sediments '99, eds. N. C. Kraus and W. G. McDougal, *4th International Symposium on Coastal Engineering and Science of Coastal Sediment Processes, Scales of Coastal Sediment Motion and Geomorphic Change*, Hauppauge, New York, United States, pp. 2010–2025.

Montello, T. M. (1992). Stratigraphy and evolution of the barrier system along the Wells — Ogunquit Embayment in Southern Maine, Unpublished MS Thesis, Boston University, Boston, MA, 220 pp.

Narr, D. F., Donahue, B. T., Berman, G. A., McIntyre, M. L., Saleem, S., Wilder, D., Jarrett, B. D., Suthard, B., Ciembronowicz, K. and Mallinson, D. J. (2003). Multibeam surveys of Egmont Deep and of sedimentary bedforms, limestone ledges, and real and artificial reefs surrounding Florida, Bahamas, and American Samoa. Coastal Sediments 2003, 9 pp.

Nwogu, O. D., Mansard, E. P. D., Miles M. D and Isaacson, M. (1987). Directional wave spectra by the maximum entropy method, IAHR Seminar, Maritime Hydraulics Section, Lausanne, Switzerland.

O'Brien, M. P. (1931). Estuary tidal prisms related to entrance areas, *Civil Engineering*, pp. 738–739.

O'Brien, M. P. (1969). Equilibrium flow areas of tidal inlets on sandy coasts, *Journal of Waterways and Harbor Division*, American Society of Civil Engineers **95** (WW1): 43–53.

Parson, L. E., Lillycrop, W. J. and McClung, J. K. (1999). Regional sediment management using high density lidar data, Coastal Sediments '99, eds. N. C. Kraus and W. G. McDougal, *4th International Symposium on Coastal Engineering and Science of Coastal Sediment Processes, Scales of Coastal Sediment Motion and Geomorphic Change*, Hauppauge, New York, United States, pp. 2445–2456.

Pierce, J. W. (1970). Tidal inlets and washover fans, *Journal of Geology* **78**: 230–234.

Pinkel, R. and Smith, J. A. (1987). Open ocean surface wave measurement using Doppler sonar, *Journal of Geophysical Research* **92**: 967–973.

Prickett, T. (1996). Coastal structure underwater inspection technologies, CETN-III-62, US Army Engineer Waterways Experiment Station, Coastal Engineering Research Center, Vicksburg, MS.

Riley, J. L. (1995). Evaluating SHOALS bathymetry using NOAA Hydrographic Survey Data, *24th Joint Meeting of UJNR Sea-Bottom Surveys Panel*, pp. 10.

Rørbæk, K. and Andersen, H. (2000). Evaluation of wave measurements with an acoustic doppler current profiler, *Oceans 2000 MST/IEEE Conference*, Providence, Rhode Island, September 11–14, 2000.

Rosati, J. D. and Kraus, N. C. (1999). Sediment budget analysis system (SBAS), Coastal and Hydraulics Engineering Technical Note IV-20, US Army Engineer Research and Development Center, Vicksburg, MS, 14 pp.

Sallenger, A. H., Jr., Krabill, W. B., Brock, J. C., Swift, R. N., Jansen, M., Manizade, S. S., Richmond, B., Hampton, M. and Eslinger, D. (1999). Airborne laser study quantifies El Nino-induced coastal change, *EOS, Transactions* **89**: 92–93.

Sha, L. P. (1989). Sand transport patterns in the ebb-tidal delta off Texel Inlet, Wadden Sea, The Netherlands, *Marine Geology* **86**: 137–154.

Sha, L. P. (1990). Surface sediments and sequence models in the ebb-tidal delta of Texel Inlet, Wadden Sea, The Netherlands, ed. L. P. Sha, *Sedimentological Studies of the Ebb-Tidal Delta along the West Friesian Islands*, The Netherlands, *Geological Ultraiectina* **64**: 95–116.

Shigemura, T. (1981). Tidal prism-throat width relationships of the Bays of Japan, Shore and Beach **49**: 34–39.

Smith, G. L. and Zarillo, G. A. (1990). Calculating long-term shoreline recession rates using aerial photographic and beach profiling techniques, *Journal of Coastal Research* **6**: 111–120.

Strong, B., Brumley B., Terray, E. A. and Kraus, N. C. (2000). Validation of the Doppler shifted dispersion relation for waves in the presence of strong tidal currents using ADCP wave directional spectra and comparison data, *6th International Workshop on Wave Hindcasting and Forecasting*, November 6–10, Monterey, CA.

Stumpf, R. P. and Holderied, K. (2003). Determination of water depth with high-resolution satellite imagery over variable bottom types, *Limnol. Oceanography* **48**: 547–556.

Speer, P.E. and Aubrey, D. G. (1985). A study of non-linear tidal propagation in shallow inlet/estuarine systems, Estuarine, Coastal, and Shelf Science **21**: 207–224.

Terray, E. A., Krogstad, H. E., Cabrera, R., Gordon, R. L. and Lohrmann, A. (1990). Measuring wave direction using upward-looking Doppler sonar, *Proc. IEEE 4th Working Conf. Current Measurement*, eds. G. F. Appell and T. B. Curtin, IEEE Press, 252–257 pp.

US Army Corps of Engineers (2001). Engineering and Design — Hydrographic Surveying, EM 1110-2-1003, US Army Corps of Engineers, Washington DC.

van Heteren, S., FitzGerald, D. M., McKinlay, P. A. and Buynevich, I. V. (1998). Radar facies of paraglacial barrier systems: Coastal New England, USA, *Sedimentology* **45**: 181–200.

Walton, T. L., Jr. and Adams, W. D. (1976). Capacity of inlet outer bars to store sand, *Proceedings 15th Coastal Engineering Conference*, American Society of Civil Engineers, Reston, VA, pp. 1, 919-1, 937.

White, S. A. and Wang, Y. (2003). Utilizing DEMs derived from LIDAR data to analize morphologic change in the North Carolinal coastline, *Remote Sensing of Environment* **85**: 39–47.

Wozencraft, J. M., Lillycrop, W. J. and Kraus, N. C. (2002). SHOALS Toolbox: Software to support visualization and analysis of large, high-density data sets, Coastal and Hydraulics Engineering Technical Note IV-43, US Army Engineer Research and Development Center, Vicksburg, MS, 8 pp.

Zarillo, G. A. (2002). Salinity distribution and flow management studies for lake worth lagoon: Final project report prepared for South Florida Water Management District, West Palm Beach, FL, 72 pp.

Zarillo, G. A. (1985). Tidal dynamics and substrate response in a salt-marsh estuary, *Marine Geology* **67**: 13–35.

Zarillo, G. A. (1982). Stability of bedforms in a tidal environment, *Marine Geology* **48**: 337–351.